Chapter 7 Dielectric Waveguides and Some Selected Topics for Photonics

Father of Optical-Fiber Communication: K. Kao (高錕)

高錕博士生於上海，其後移居香港，肄業於聖約瑟書院。他在英國取得倫敦大學理學士和哲學博士學位，歷任歐美多家著名電訊機構及實驗室的重要職位，也是香港中文大學前校長。他在 1966 年發表論文，提出如何實現以玻璃纖維作為導體，令光代替電流傳遞訊息，引進光通信的時代，因此被譽為「**光纖通訊之父**」，2009 年獲得諾貝爾物理獎。

Father of Integrated Optics: P. K. Tien (田炳耕)

田炳耕博士，浙江上虞人，1919 年生，美國工程院院士和美國科學院院士。他在上海中法工專畢業後，於 1937 年考入重慶國立中央大學電機工程系，1940 年因足傷返滬，轉讀上海交通大學，於 1941 年畢業。1947 年田炳耕去美國史丹福(Stanford)大學完成博士課程，在 Stanford 大學發明了微波放大的新元件空間電荷波放大器(Space charge wave Amplifier)，該放大器公佈在 1952 年美國 Proceeding of IRE 的第 40 卷 688 頁上。1952 年田炳耕與當時就讀於 Stanford 大學經濟系的陳南茜結婚，並進入美國貝爾實驗室(Bell Lab)工作，發表了多篇研究論文，並取得多項專利。這些論文和專利涉及微波理論和技術、材料科學、電波傳播、雜訊理論、鐵磁體、超導體、聲電效應，雷射物理、積體光學、高速電子學等。1975 年田炳耕當選為美國工程院院士，1978 年又當選為美國科學院院士。田炳耕博士被譽為「**積體光學之父**」。

Godfather of A-O Devices: C. S. Tsai (蔡振水)

蔡振水博士，1935 年生，1957 年畢業於台灣大學電機工程系，1965 年獲得美國史丹福大學電機工程博士。隨後在洛克希德飛機飛彈公司研究中心（Lockheed Palo Alto Research Center）工作三年半，1969 年應聘美國卡乃基美濃大學（Carnegie-Mellon University）電機工程系助理教授，1974 年晉昇正教授，並於 1979 年膺得傑出教授。蔡博士 1980 年應聘加州大學爾灣分校(Univ. of Calif., Irvine)電機工程系資深教授，1985 年擔任系主任一年半，並於 1991 年榮膺傑出教授。蔡主任之研究領域包括積體聲光學、積體磁光學、磁性微波元件、超音波顯微學等，論文及專著豐富，並獲得教研獎賞十多項。

Godfather of Nonlinear Optics: Y. R. Shen (沈元壤)

沈元壤博士生於 1935 年，台灣大學電機學士、美國史丹福大學碩士、哈佛大學博士，曾任加州大學柏克萊分校助教授、副教授，於 1970 年升任教授；1964 年起任該校勞倫斯實驗室材料化學科學組計畫主持人，1984 年起加入該校超級材料中心研究計畫擔任主持人。沈院士曾獲查理湯斯獎(Charles Tomes Award)、非線性光學最高獎、美國能源部固態物理特殊科學成就獎、勞倫斯柏克萊傑出技術轉移獎等殊榮。1989 年其大作 Introduction to Nonlinear Optics 獲獎，並獲得美國多層光學記憶系體專利。民國 1990 年當選中研院十八屆院士。

Godfather of Optoelectronic Engineering: C. L. Tang(湯仲良)

湯仲良博士生於 1934 年 5 月 14 日，1955 年獲得華盛頓大學學士，1956 年獲得加州理工學院(California Institute of Technology)碩士，1960 年獲得哈佛大學博士。1964 年後任教康乃爾大學，為世界著名的光電專家，1987 年當選美國國家工程學院院士，1994 年並當選第二十屆中研院院士。

Famous Scholar of Optoelectronics: Pochi Yeh (葉伯琦)

葉伯琦博士著有 Optical waves in layered media、Optical waves in crystals (與 Yariv 合著)等光電經典著作，為世界級著名的光電學者。

7-1 Introduction to Integrated Optics

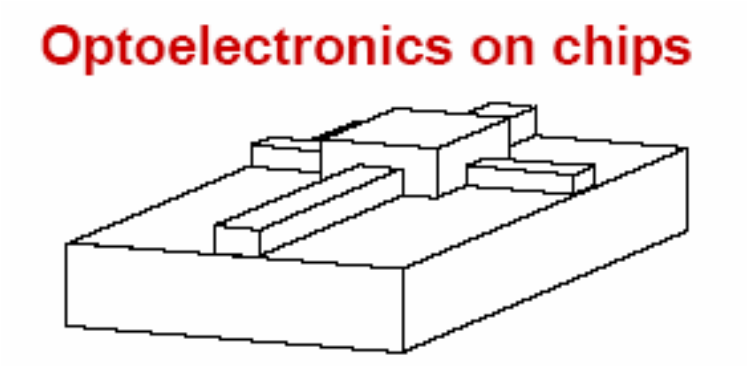

Optical switch: It is a combination of waveguide devices and electrodes to control the intensity of light.

KTN switch constructed using KTN and silica waveguides.
Optical ports can be switched by applying voltage to electrode.

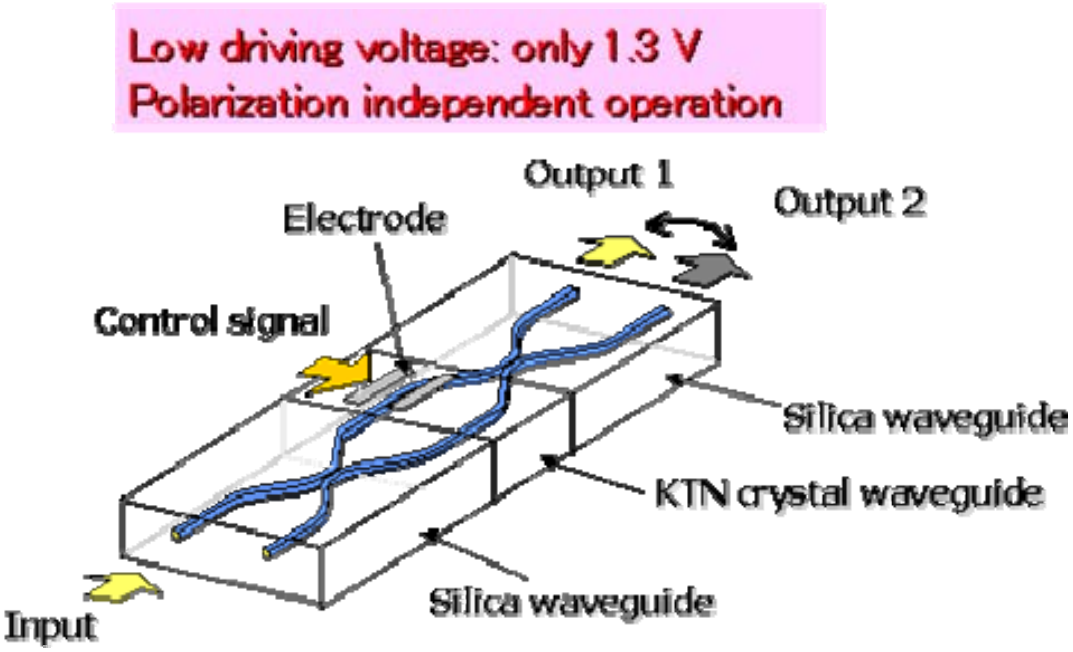

7-2 Basic Integrated Optoelectronic Devices

Mach-Zender interferometer:

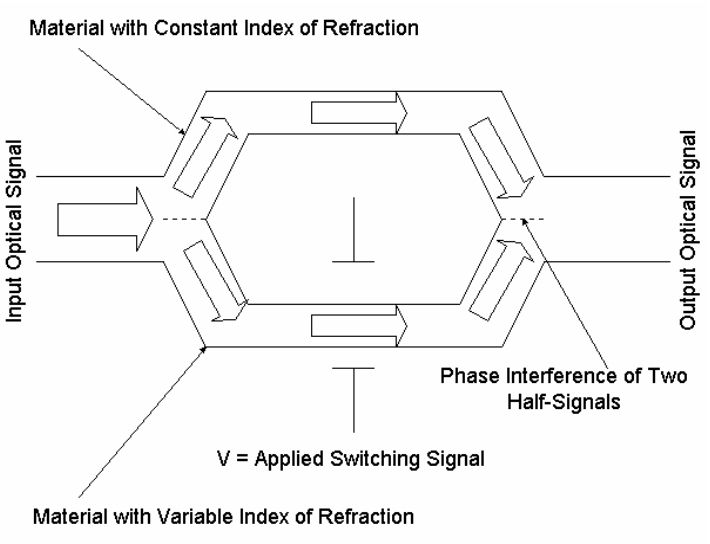

Eg. Application of Mach-Zehnder interferometer: An electro-optic switch in optical fiber communications.

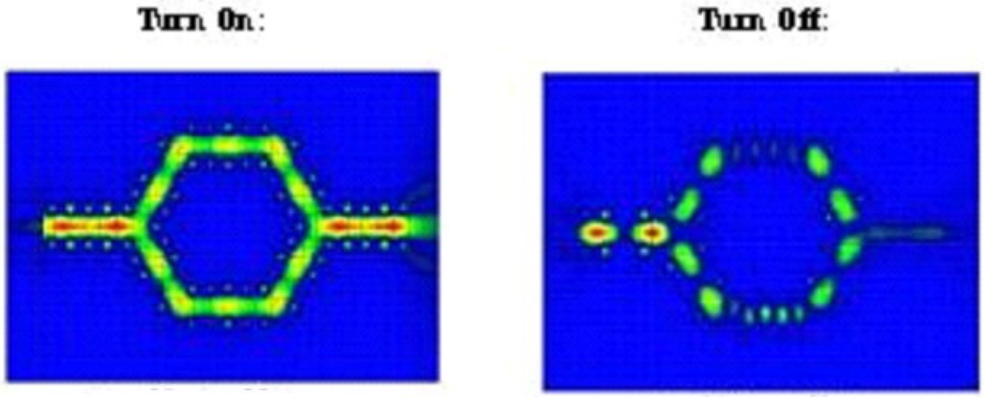

Optical directional coupler:

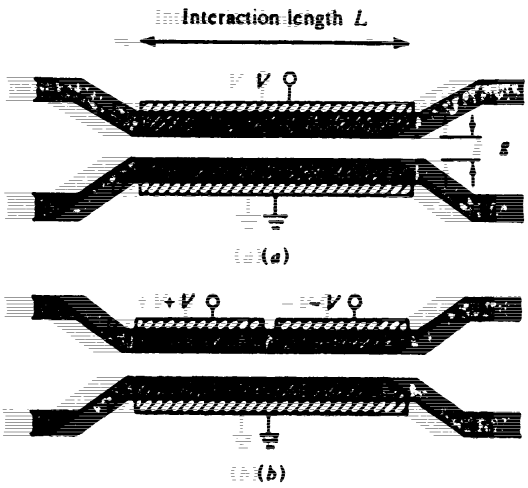

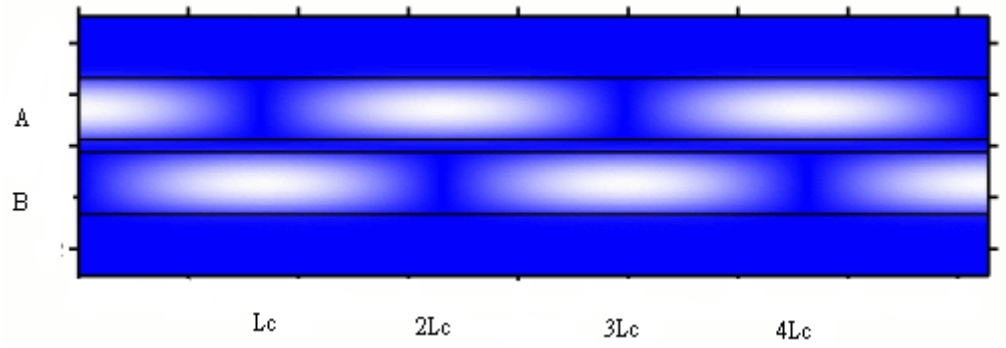

Coupled mode equations: The *E*-fields of two identical waveguides *A* and *B* fulfill

$$\begin{cases} \dfrac{dE_A}{dz} = -j\beta E_A - j\kappa E_B \\ \dfrac{dE_B}{dz} = -j\beta E_B - j\kappa E_A \end{cases}, \quad \begin{cases} E_A(0) = 1 \\ E_B(0) = 0 \end{cases},$$ where ***κ*** is **the coupling coefficient**. The solutions of the coupled mode equations are $E_A(z) = \cos(\kappa z)e^{-j\beta z}$ and $E_B(z) = -j\sin(\kappa z)e^{-j\beta z}$, respectively**.** And **the coupling length** is $L_c = \pi/2\kappa$. While the waveguiding mode traverses a distance of odd multiple of the coupling length (L_c, $3L_c$, $5L_c$, …, etc), the optical power is completely transferred into the other waveguide. But it is back after a distance of **even multiple of the coupling lengths** ($2L_c$, $4L_c$, $6L_c$, …, etc). If the waveguiding mode traverses a distance of **odd multiple of the half coupling length** ($L_c/2$, $3L_c/2$, $5L_c/2$, …, etc), the optical power is equally distributed in the two guides,

Eg. A 3-dB optical power splitter based on directional coupler by the setting the length of coupling region=$L_c/2$.

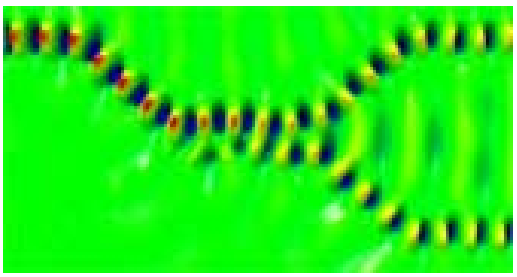

Eg. A wavelength multiplexer/demultiplexer using photonic crystal waveguides.

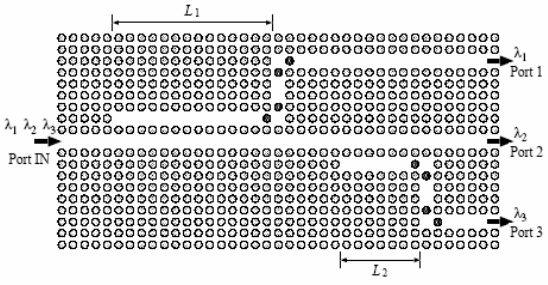

wavelength λ/a	extinction ratio [dB]	insertion loss [dB]	output
2.66	>20.6	6.4×10^{-3}	Port 1
2.58	>20.5	3.8×10^{-2}	Port 2
2.72	>17.9	8.1×10^{-2}	Port 3

(a)

(b)

(c)

***X*-type switch:** Utilize the voltage to control the refractive index of the cross region and vary the reflectance of light in this region.

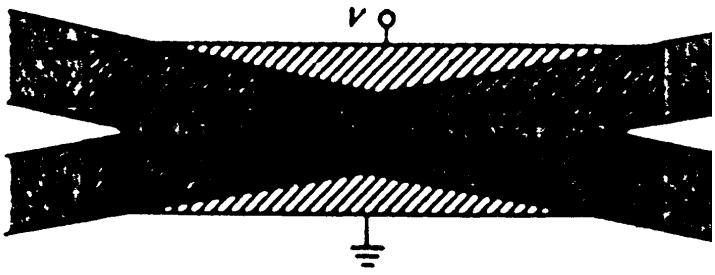

Integrated-optical microwave spectrum analyzer: It enables the pilot of a military aircraft to obtain an instantaneous spectral analysis of an incoming radar beam to determine whether or not his plane is being tracked by the enemy's ground station, air-to-air missile, and so on. It is an Example of SAW (Surface acoustic wave) Device.

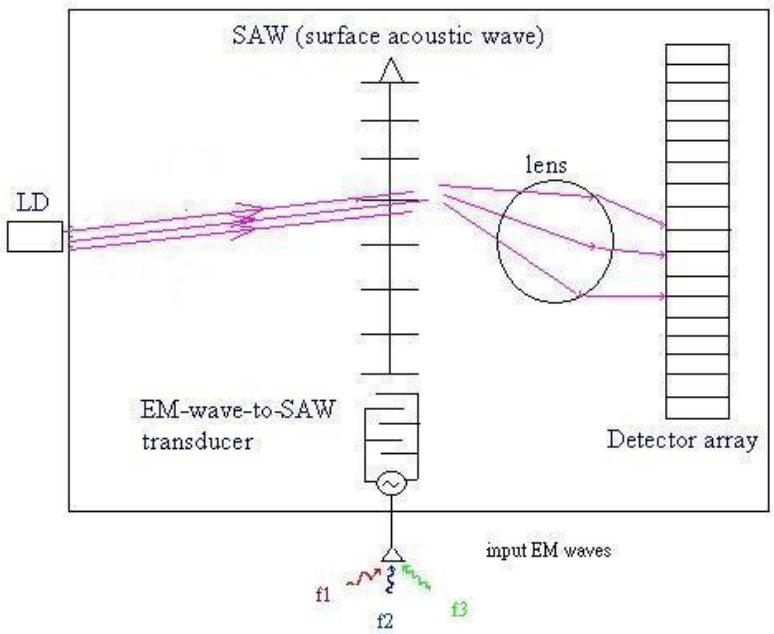

Another application of the above SAW device—Laser beam alignment Controller of the CD/VCD/DVD/CD-ROM R/W head: If one change the frequency of the incoming EM wave to the SAW transducer, the output direction of the laser beam can be varied.

MMI (Multi-mode interference) waveguide devices: A section of wide waveguide for exciting multi-modes. It is usually utilized an optical splitter, an optical combiner, an optical filter, and an all-optical logic gate, etc.

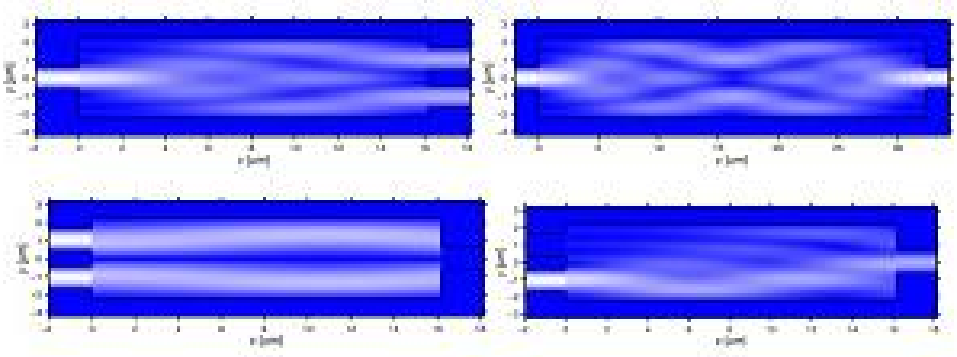

Eg. An example of all-optical logic gate with an MMI waveguide:

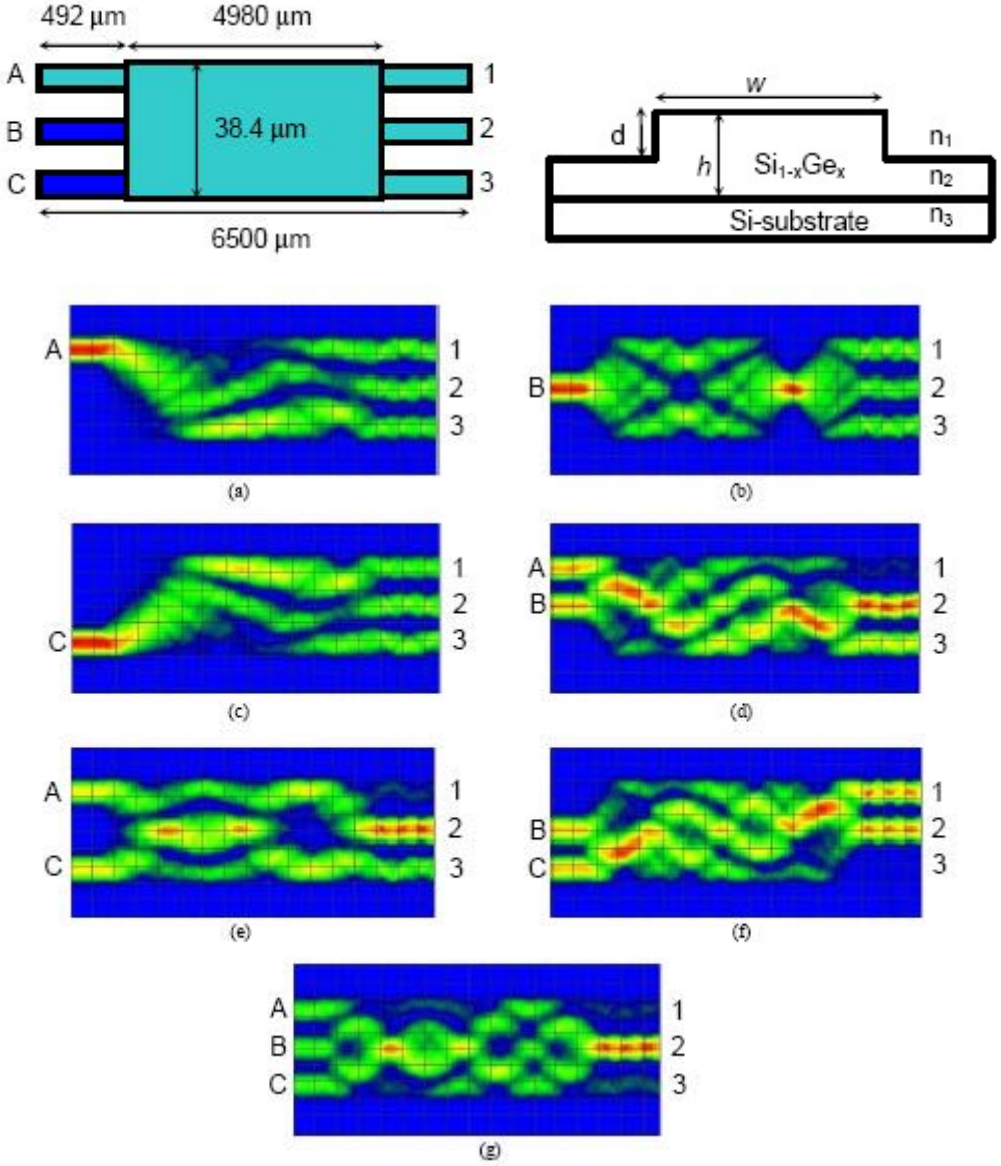

OR Logic Gate

Input signal	A	0	1	0	0	1	1	0	1
	B	0	0	1	0	1	0	1	1
	C	0	0	0	1	0	1	1	1
Comparison Fig.			(a)	(b)	(c)	(d)	(e)	(f)	(g)
Output signal in port 2		0	1	1	1	1	1	1	1

NAND Logic Gate

Input signal	A	1	1	1	1
Control pulse	B	0	1	0	1
	C	0	0	1	1
Comparison Fig.		(a)	(d)	(e)	(g)
Output signal in port 3		1	1	1	0

NOT Logic Gate

Control pulse	A	0	1
Input signal	B	1	1
Comparison Fig.		(b),(f)	(d),(g)
Output signal in port 1		1	0

Table NOT Logic Gate

Control pulse	C	0	1
Input signal	B	1	1
Comparison Fig.		(b),(d)	(f),(g)
Output signal in port 3		1	0

Table NOT Logic Gate

Control pulse	A	0	1
Input signal	C	1	1
Comparison Fig.		(c),(f)	(e),(g)
Output signal in port 1		1	0

Table NOT Logic Gate

Control pulse	B	0	1
Input signal	C	1	1
Comparison Fig.		(c),(e)	(f),(g)
Output signal in port 3		1	0

Table NOR Logic Gate

Input signal	A	1	1	1	1
Control pulse	B	0	1	0	1
	C	0	0	1	1
Comparison Fig.		(a)	(d)	(e)	(g)
Output signal in port 1		1	0	0	0

Eg. Propagation along periodical dielectric waveguides. (by Dr. G. D. Chang, 張高德博士)

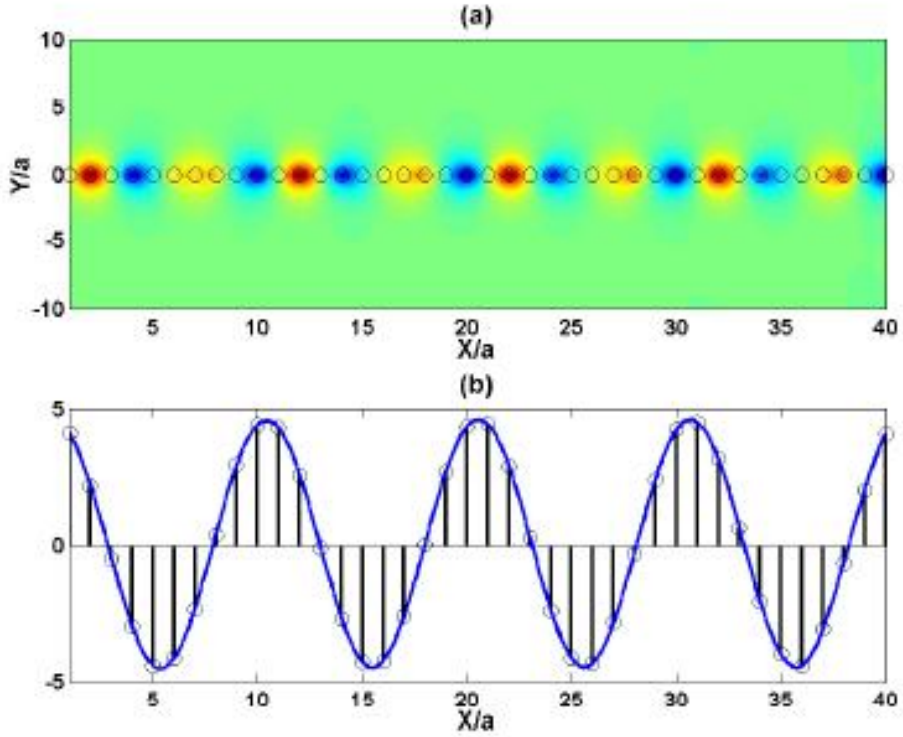

(a) The snapshot of **E**-field pattern (the real part of the complex amplitude) for the mode with frequency $\omega = 0.25(2\pi c/a)$ and Bloch wavevector $\mathbf{k} = 0.4(2\pi/a)\hat{\mathbf{x}}$. (b) The field pattern in (a), when multiplied by the factor $(-1)^n$ and evaluated at the center of the nth cylinder, fits to a sinusoidal wave. The wavelength is about $10a$.

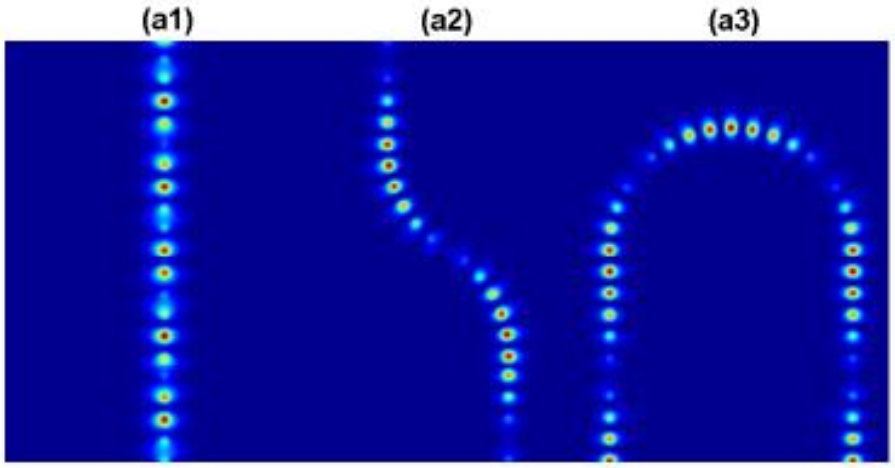

Three types of bent waveguides. (a1) A straight waveguide without any bend. (a2) An S-shaped waveguide formed by combining two 45°-bent waveguides. (a3) A U-shaped waveguide formed by combining two 90°-bent waveguides. Transmission in these waveguides is higher than 90% when the working frequency is chosen as $\omega = 0.25(2\pi c/a)$

Micro-diffractive device (by Dr. J. –R. Sze, 施至柔博士):

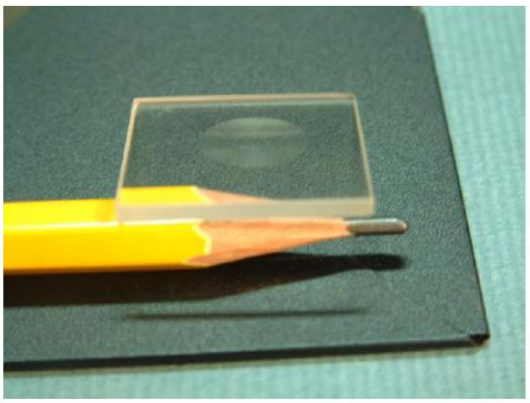

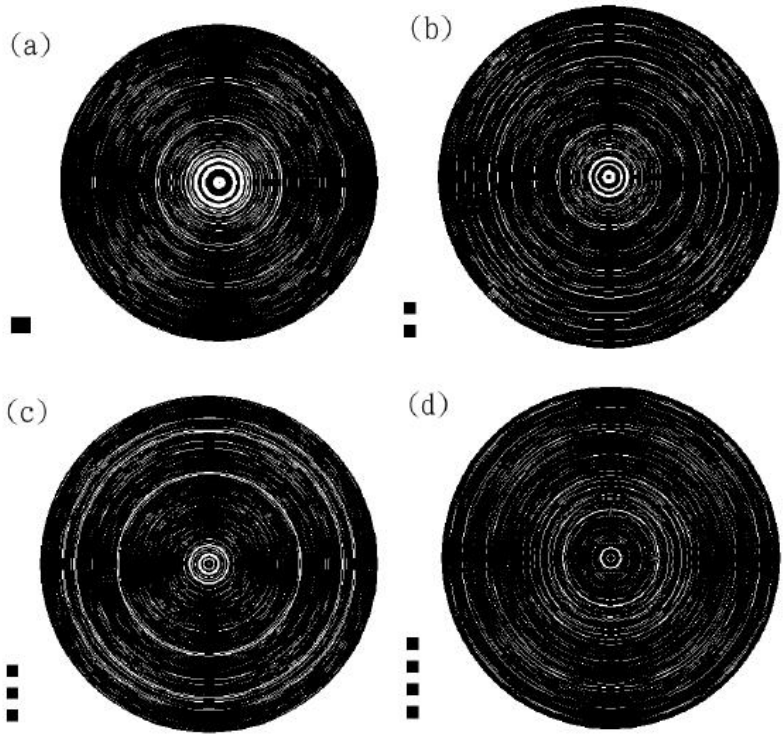

製作十六階繞射元件所使用的光罩

(a)第一道光罩；(b)第二道光罩；(c)第三道光罩(d)第四道光罩。

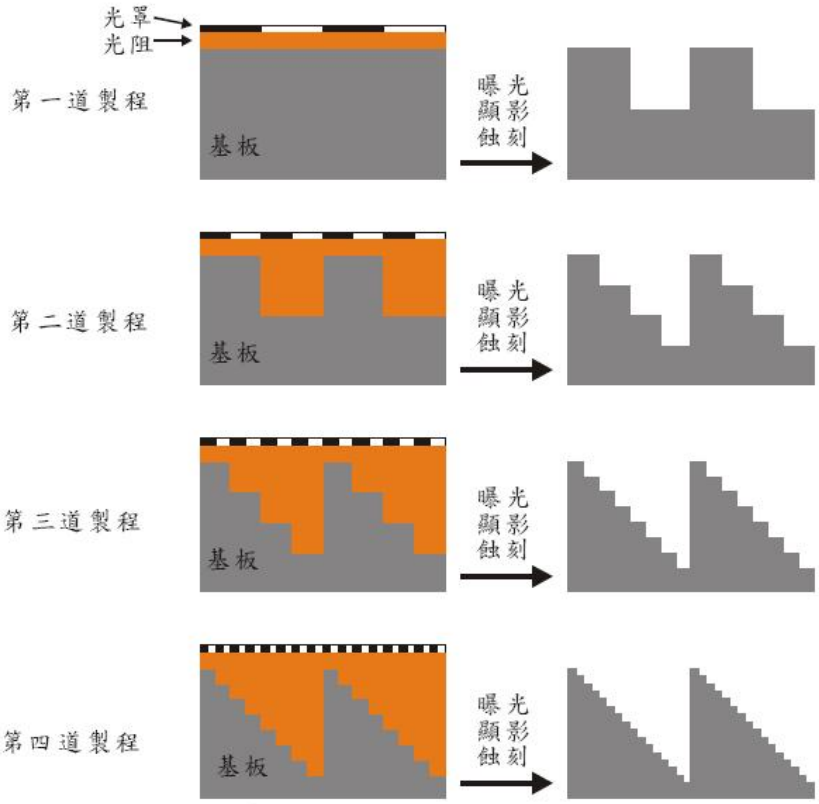

製作十六階繞射元件的基本概念圖

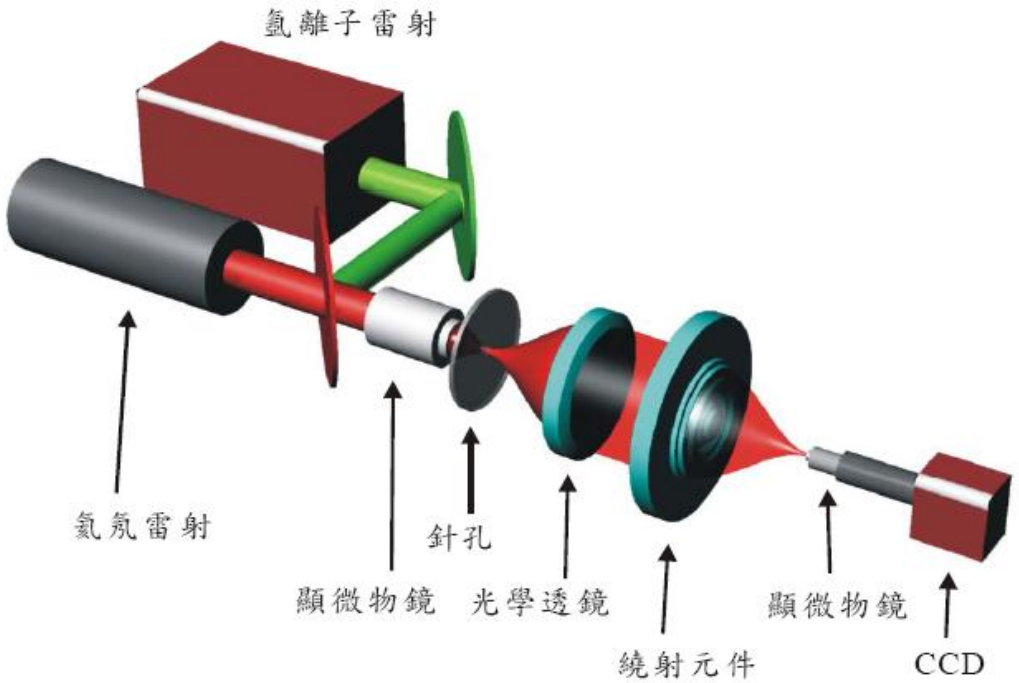

十六階繞射元件的光學特性量測設備架構圖。

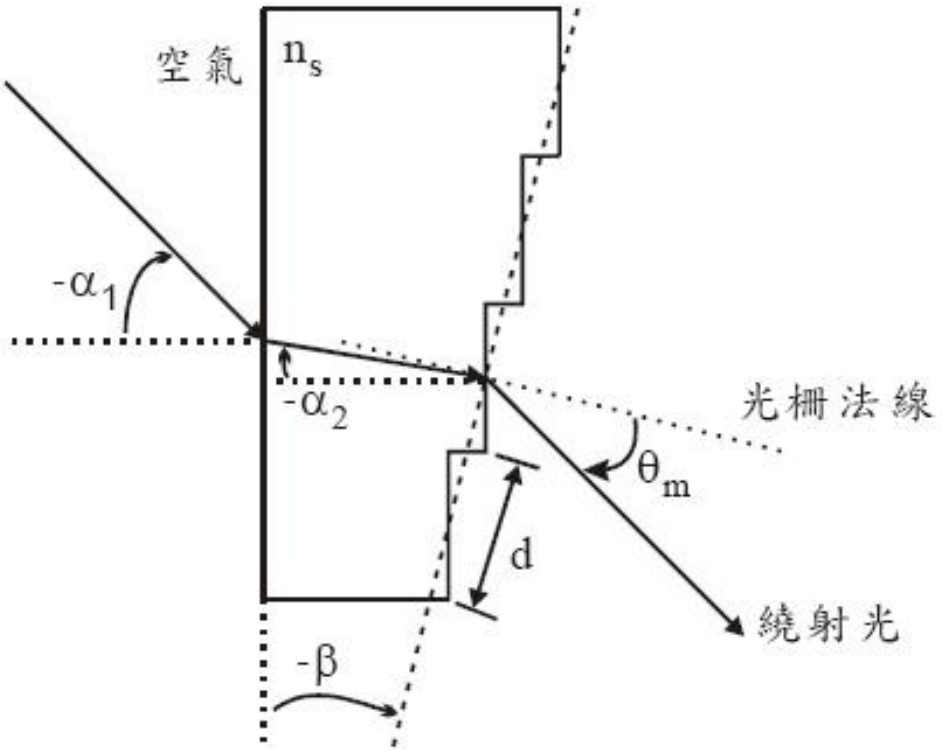

稜鏡光柵示意圖

(a)

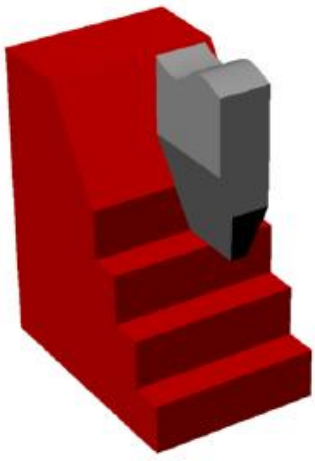

(b)

（此照片由工研院機械所提供）

以鑽石微加工技術製作稜鏡光柵示意圖
（a）工作機台照片，（b）稜鏡光柵加工示意圖

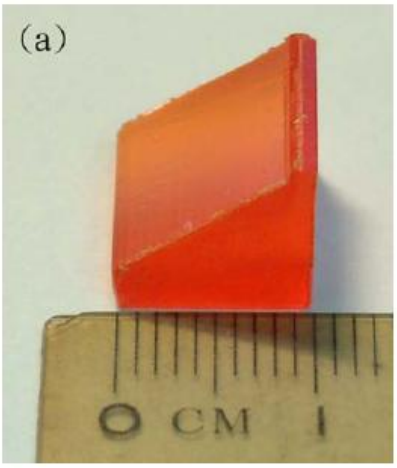

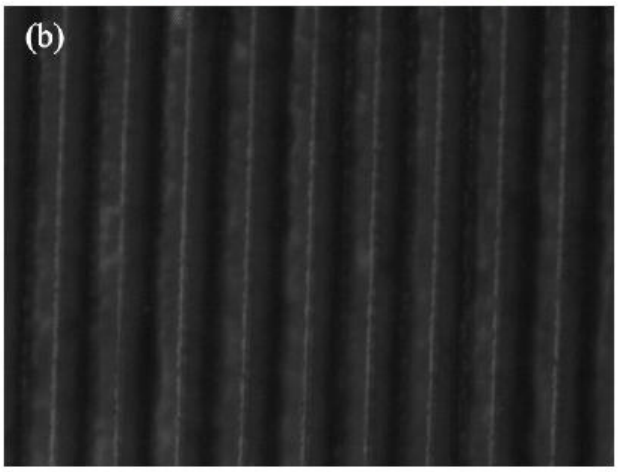

製作完成的稜鏡光柵。 (a) 實體照片。(b) 部分光柵放大照片

7-3 Dielectric–Slab Waveguides in the Free Space

***Case 1 TM modes*: H_z=0**

$$\frac{d^2E_z^0(y)}{dy^2}+h^2E_z^0(y)=0,\ h^2=\gamma^2+\omega^2\mu\varepsilon,\ \gamma=j\beta$$

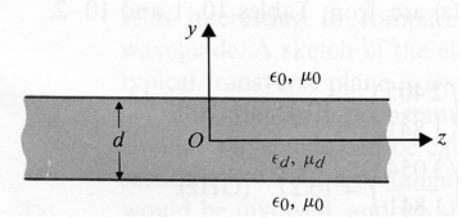

$$\Rightarrow E_z^0(y)=\begin{cases} C_u e^{-\alpha(y-\frac{d}{2})}, & y\ge\frac{d}{2} \\ E_o\sin k_y y+E_e\cos k_y y, & |y|\le\frac{d}{2} \\ C_e e^{\alpha(y+\frac{d}{2})}, & y\le-\frac{d}{2} \end{cases},\quad \begin{aligned} k_y^{\ 2}&=\omega^2\mu_d\varepsilon_d-\beta^2=h_d^2 \\ \alpha^2&=\beta^2-\omega^2\mu_0\varepsilon_0=-h_0^2 \end{aligned}$$

At cutoff: $\alpha\to0$, $\beta^2\to\omega^2\mu_0\varepsilon_0$, waves are no longer bound to the waveguide

Above cutoff: $\omega\sqrt{\mu_0\varepsilon_0}<\beta<\omega\sqrt{\mu_d\varepsilon_d}$

Surface impedance of TM mode: $Z_s=-\dfrac{E_z^0}{H_x^0}=j\dfrac{\alpha}{\omega\varepsilon_0}$ (TM)

And $E_z^0(y)$ is continuous at $y=\pm\dfrac{d}{2}\Rightarrow$ Relationship among E_o, E_e, C_o, and C_e.

***Odd TM mode* ($E_o\neq0$, $E_e=0$):**

(1) $|y|\le d/2$: (2) $y\ge d/2$: (3) $y\le -d/2$:

$$\begin{cases} E_z^0(y)=E_o\sin k_y y \\ E_y^0(y)=-\dfrac{j\beta}{k_y}E_o\cos k_y y \\ H_x^0(y)=\dfrac{j\omega\varepsilon_d}{k_y}E_o\cos k_y y \end{cases}\quad \begin{cases} E_z^0(y)=(E_o\sin\dfrac{k_y d}{2})e^{-\alpha(y-d/2)} \\ E_y^0(y)=-\dfrac{j\beta}{\alpha}(E_o\sin\dfrac{k_y d}{2})e^{-\alpha(y-d/2)} \\ H_x^0(y)=\dfrac{j\omega\varepsilon_0}{\alpha}(E_o\sin\dfrac{k_y d}{2})e^{-\alpha(y-d/2)} \end{cases}\quad \begin{cases} E_z^0(y)=-(E_o\sin\dfrac{k_y d}{2})e^{\alpha(y+d/2)} \\ E_y^0(y)=-\dfrac{j\beta}{\alpha}(E_o\sin\dfrac{k_y d}{2})e^{\alpha(y+d/2)} \\ H_x^0(y)=\dfrac{j\omega\varepsilon_0}{\alpha}(E_o\sin\dfrac{k_y d}{2})e^{\alpha(y+d/2)} \end{cases}$$

$H_x^0(y)$ is continuous at $y=\dfrac{d}{2}\Rightarrow\dfrac{\alpha}{k_y}=\dfrac{\varepsilon_0}{\varepsilon_d}\tan\dfrac{k_y d}{2}$ (Odd TM)

$$\alpha^2+h_y^2=\omega^2(\mu_d\varepsilon_d-\mu_0\varepsilon_0)\Rightarrow[\omega^2(\mu_d\varepsilon_d-\mu_0\varepsilon_0)-k_y^2]^{1/2}=\frac{\varepsilon_0}{\varepsilon_d}h_y\tan\frac{k_y d}{2}$$

***Even TM mode* (E_o=0, E_e≠0):**

(1) $|y| \le d/2$: (2) $y \ge d/2$: (3) $y \le -d/2$:

$$\begin{cases} E_z^0(y) = E_e \cos k_y y \\ E_y^0(y) = \dfrac{j\beta}{k_y} E_e \sin k_y y \\ H_z^0(y) = -\dfrac{j\omega\varepsilon_d}{k_y} E_e \sin k_y y \end{cases} \quad \begin{cases} E_z^0(y) = (E_e \cos\dfrac{k_y d}{2}) e^{-\alpha(y-d/2)} \\ E_y^0(y) = -\dfrac{j\beta}{\alpha}(E_e \cos\dfrac{k_y d}{2}) e^{-\alpha(y-d/2)} \\ H_z^0(y) = \dfrac{j\omega\varepsilon_0}{\alpha}(E_e \cos\dfrac{k_y d}{2}) e^{-\alpha(y-d/2)} \end{cases} \quad \begin{cases} E_z^0(y) = (E_e \cos\dfrac{k_y d}{2}) e^{\alpha(y+d/2)} \\ E_y^0(y) = \dfrac{j\beta}{\alpha}(E_e \cos\dfrac{k_y d}{2}) e^{\alpha(y+d/2)} \\ H_z^0(y) = -\dfrac{j\omega\varepsilon_0}{\alpha}(E_e \cos\dfrac{k_y d}{2}) e^{\alpha(y+d/2)} \end{cases}$$

$H_z^0(y)$ is continuous at $y = \dfrac{d}{2} \Rightarrow \dfrac{\alpha}{k_y} = -\dfrac{\varepsilon_0}{\varepsilon_d} \cot\dfrac{k_y d}{2}$ (Even TM)

Odd TM Modes	Even TM Modes
$\tan\left(\dfrac{\omega_{co} d}{2}\sqrt{\mu_d\epsilon_d - \mu_0\epsilon_0}\right) = 0$	$\cot\left(\dfrac{\omega_{ce} d}{2}\sqrt{\mu_d\epsilon_d - \mu_0\epsilon_0}\right) = 0$
$\pi f_{co} d\sqrt{\mu_d\epsilon_d - \mu_0\epsilon_0} = (n-1)\pi,$ $n = 1, 2, 3, \ldots$	$\pi f_{ce} d\sqrt{\mu_d\epsilon_d - \mu_0\epsilon_0} = (n-\frac{1}{2})\pi,$ $n = 1, 2, 3, \ldots$
$\boxed{f_{co} = \dfrac{(n-1)}{d\sqrt{\mu_d\epsilon_d - \mu_0\epsilon_0}}}$ (10–264)	$\boxed{f_{ce} = \dfrac{(n-\frac{1}{2})}{d\sqrt{\mu_d\epsilon_d - \mu_0\epsilon_0}}}$ (10–265)

***Case 2 TE modes*: E_z=0**

$$\frac{d^2H_z^0(y)}{dy^2}+h^2H_z^0(y)=0,\quad h^2=\gamma^2+\omega^2\mu\varepsilon,\quad \gamma=j\beta$$

$$H_z^0(y)=\begin{cases} C_u'e^{-\alpha(y-\frac{d}{2})}, & y\ge\frac{d}{2} \\ H_o\sin k_y y+H_e\cos k_y y, & |y|\le\frac{d}{2} \\ C_e'e^{\alpha(y+\frac{d}{2})}, & y\le-\frac{d}{2} \end{cases}$$

Surface impedance of TE mode: $Z_s=\dfrac{E_x^0}{H_z^0}=-j\dfrac{\omega\mu_0}{\alpha}$ (TE)

***Odd TE mode* ($H_o\neq0$, H_e=0):**

(1) $|y|\le d/2$: (2) $y\ge d/2$: (3) $y\le -d/2$:

$$\begin{cases} H_z^0(y)=H_o\sin k_y y \\ H_y^0(y)=-\dfrac{j\beta}{k_y}H_o\cos k_y y \\ E_x^0(y)=-\dfrac{j\omega\mu_d}{k_y}H_o\cos k_y y \end{cases},\quad \begin{cases} H_z^0(y)=(H_o\sin\dfrac{k_y d}{2})e^{-\alpha(y-d/2)} \\ H_y^0(y)=-\dfrac{j\beta}{\alpha}(H_o\sin\dfrac{k_y d}{2})e^{-\alpha(y-d/2)} \\ E_x^0(y)=-\dfrac{j\omega\mu_0}{\alpha}(H_o\sin\dfrac{k_y d}{2})e^{-\alpha(y-d/2)} \end{cases},\quad \begin{cases} H_z^0(y)=-(H_o\sin\dfrac{k_y d}{2})e^{\alpha(y+d/2)} \\ H_y^0(y)=-\dfrac{j\beta}{\alpha}(H_o\sin\dfrac{k_y d}{2})e^{\alpha(y+d/2)} \\ E_x^0(y)=-\dfrac{j\omega\mu_0}{\alpha}(H_o\sin\dfrac{k_y d}{2})e^{\alpha(y+d/2)} \end{cases}$$

$E_x^0(y)$ is continuous at $y=\dfrac{d}{2}\Rightarrow\dfrac{\alpha}{k_y}=\dfrac{\mu_0}{\mu_d}\tan\dfrac{k_y d}{2}$ (Odd TE)

***Even TE mode* (H_o=0, $H_e\neq0$):**

(1) $|y|\le d/2$: (2) $y\ge d/2$: (3) $y\le -d/2$:

$$\begin{cases} H_z^0(y)=H_e\cos k_y y \\ H_y^0(y)=\dfrac{j\beta}{k_y}H_e\sin k_y y \\ E_x^0(y)=\dfrac{j\omega\mu_d}{k_y}H_e\sin k_y y \end{cases},\quad \begin{cases} H_z^0(y)=(H_e\cos\dfrac{k_y d}{2})e^{-\alpha(y-d/2)} \\ H_y^0(y)=-\dfrac{j\beta}{\alpha}(H_e\cos\dfrac{k_y d}{2})e^{-\alpha(y-d/2)} \\ E_x^0(y)=-\dfrac{j\omega\mu_0}{\alpha}(H_e\cos\dfrac{k_y d}{2})e^{-\alpha(y-d/2)} \end{cases},\quad \begin{cases} H_z^0(y)=(H_e\cos\dfrac{k_y d}{2})e^{\alpha(y+d/2)} \\ H_y^0(y)=\dfrac{j\beta}{\alpha}(H_e\cos\dfrac{k_y d}{2})e^{\alpha(y+d/2)} \\ E_x^0(y)=\dfrac{j\omega\varepsilon_0}{\alpha}(H_e\cos\dfrac{k_y d}{2})e^{\alpha(y+d/2)} \end{cases}$$

$E_x^0(y)$ is continuous at $y=\dfrac{d}{2}\Rightarrow\dfrac{\alpha}{k_y}=-\dfrac{\mu_0}{\mu_d}\cot\dfrac{k_y d}{2}$ (Even TE)

Characteristic Relations for Dielectric-Slab Waveguide†

Mode		Characteristic Relation	Cutoff Frequency
TM	Odd	$(\alpha/k_y)=(\epsilon_0/\epsilon_d)\tan(k_y d/2)$	$f_{co}=(n-1)/d\sqrt{\mu_d\epsilon_d-\mu_0\epsilon_0}$
	Even	$(\alpha/k_y)=-(\epsilon_0/\epsilon_d)\cot(k_y d/2)$	$f_{ce}=(n-\frac{1}{2})/d\sqrt{\mu_d\epsilon_d-\mu_0\epsilon_0}$
TE	Odd	$(\alpha/k_y)=(\mu_0/\mu_d)\tan(k_y d/2)$	$f_{co}=(n-1)/d\sqrt{\mu_d\epsilon_d-\mu_0\epsilon_0}$
	Even	$(\alpha/k_y)=-(\mu_0/\mu_d)\cot(k_y d/2)$	$f_{ce}=(n-\frac{1}{2})/d\sqrt{\mu_d\epsilon_d-\mu_0\epsilon_0}$

† $\alpha=[\omega^2(\mu_d\epsilon_d-\mu_0\epsilon_0)-k_y^2]^{1/2}$.

Eg. A dielectric-slab waveguide with $\mu_d=\mu_0$ and $\varepsilon_d=2.5\varepsilon_0$ is situated in free space. Determine the minimum thickness of the slab so that a TM or TE wave of the even type at a frequency 20*GHz* may propagate along the guide.

(Sol.) The lowest TM and TE waves of even type have the same cutoff frequency:

$$f_c=\frac{n-(1/2)}{d\sqrt{\mu_d\varepsilon_d-\mu_0\varepsilon_0}}$$

For n=1, $f_c=\dfrac{c}{2d\sqrt{(\mu_d\varepsilon_d/\mu_0\varepsilon_0)-1}}$, $d_{\min}=\dfrac{c}{2f_c\sqrt{(\mu_d\varepsilon_d/\mu_0\varepsilon_0)-1}}=6.12\times10^{-3}\,m$.

Eg. A waveguide consists of an infinite dielectric slab (μ_d,ε_d) of thickness *d* that is sitting on a perfect conductor. (a) What are the propagating modes and what are their cutoff frequencies? (b) Obtain the phasor expressions for the surface current and surface charge densities on the conducting base for the propagating modes.

(Sol.) (a) Odd TM and Odd TE modes exist. $(f_c)_{odd-TM}=\dfrac{n-1}{2d\sqrt{\mu_d\varepsilon_d-\mu_0\varepsilon_0}}$,

$$(f_c)_{odd-TE}=\frac{n-1}{2d\sqrt{\mu_d\varepsilon_d-\mu_0\varepsilon_0}}$$

(b) Odd TM: $\begin{cases}E_y^0(y)=-\dfrac{j\beta}{k_y}E_0\cos k_y y\\ H_x^0(y)=\dfrac{j\omega\varepsilon_d}{k_y}E_0\cos k_y y\end{cases}\Rightarrow\begin{cases}\bar{J}_s=-\hat{y}\times\bar{H}(0)=-\hat{z}\dfrac{j\omega\varepsilon_d}{k_y}E_0\\ \rho_s=\hat{y}\cdot\varepsilon_d\bar{E}_y(0)=-\dfrac{j\beta\varepsilon_d}{k_y}E_0\end{cases}$

Eg. Find the solution of with $\alpha d/2$ versus for d=1*cm* and ε_r=3.25 if (a) f=200*MHz*, and (b) f=500*MHz*. Determine β and α for the lowest-order odd TM modes at the two frequencies.

(Sol.) Solve $\begin{cases}\alpha^2+k_y^{\,2}=\omega^2(\mu_d\varepsilon_d-\mu_0\varepsilon_0)\\ \dfrac{\alpha}{k_y}=\dfrac{\varepsilon_0}{\varepsilon_d}\tan\dfrac{k_y d}{2}\end{cases}$ by numerical methods.

(a) f=200×10^6*Hz*, ω=4π10^8 ⇒ α=0.061*Np/m*, k_y=6.28*rad/m*, $\beta=\sqrt{\omega^2\mu_d\varepsilon_d-k_y^{\,2}}$=4.19*rad/m*, f=200×10^6*Hz*

(b) f=500×10^6*Hz*, ω=π10^9 ⇒ α=0.38*Np/m*, β=10.48 *rad/m*

7-4 Optical Fibers

Consider a z-directional optical fiber with $n(r)=\begin{cases} n_1, & r \le a \\ n_2, & r > a \end{cases}$, where n_1 and n_2 ($n_1>n_2$.) are the refractive indices of the core and the cladding regions, respectively. In the optical frequency band, $n_1=\sqrt{\varepsilon_{r1}}$ and $n_2=\sqrt{\varepsilon_{r2}}$.

Classification of optical fibers:

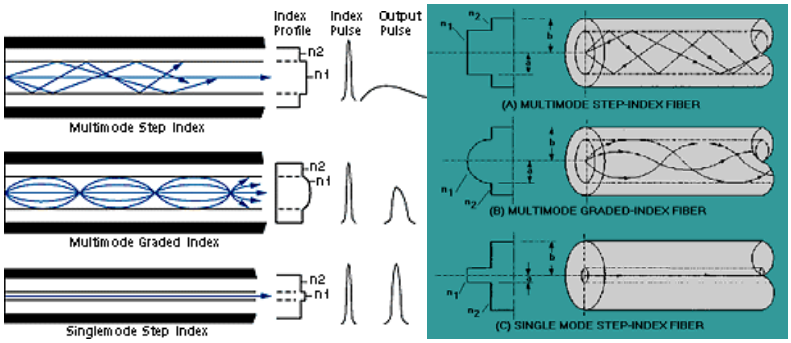

Case 1 Step-index fiber: n_1 and n_2 are constants.

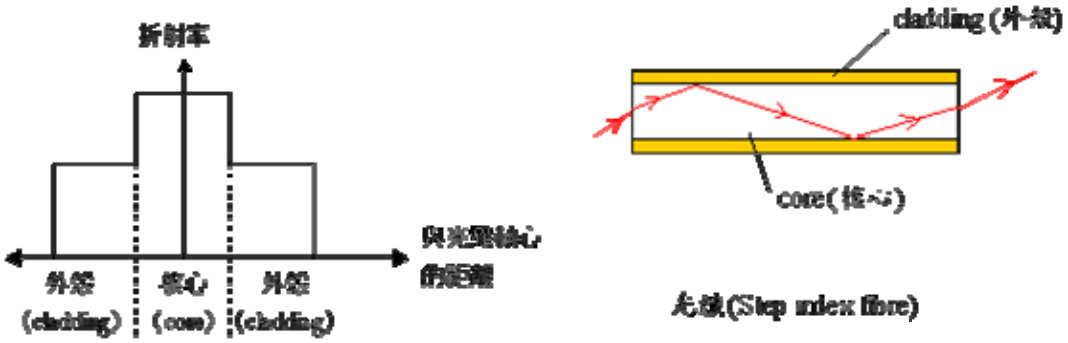

In this case, no pure TE and TM modes exist. The waveguiding modes become the hybrid eigenmodes (the $\boldsymbol{EH_{lm}}$ and the $\boldsymbol{HE_{lm}}$ modes). The field components are obtained by solving $(\nabla_t^2+h^2)E_z=\frac{1}{r}\frac{\partial}{\partial r}(r\frac{\partial E_z}{\partial r})+\frac{1}{r^2}\frac{\partial^2 E_z}{\partial \phi^2}+h^2E_z=0$,

$$(\nabla_t^2+h^2)H_z=\frac{1}{r}\frac{\partial}{\partial r}(r\frac{\partial H_z}{\partial r})+\frac{1}{r^2}\frac{\partial^2 H_z}{\partial \phi^2}+h^2H_z=0,$$

and $\begin{cases} E_r=-\frac{j}{h^2}[\beta\frac{\partial E_z}{\partial r}+\frac{\omega\mu}{r}\frac{\partial H_z}{\partial \phi}], \quad H_r=\frac{j}{h^2}[\frac{\omega\varepsilon}{r}\frac{\partial E_z}{\partial \phi}-\beta\frac{\partial H_z}{\partial r}] \\ E_\phi=\frac{j}{h^2}[-\frac{\beta}{r}\frac{\partial E_z}{\partial \phi}+\omega\mu\frac{\partial H_z}{\partial r}], \quad H_\phi=-\frac{j}{h^2}[\omega\varepsilon\frac{\partial E_z}{\partial r}+\frac{\beta}{r}\frac{\partial H_z}{\partial \phi}] \end{cases}$.

The solutions are $E_z = \begin{cases} AJ_l(hr)e^{j(l\phi-\beta z)}, & r \le a \\ CK_l(hr)e^{j(l\phi-\beta z)}, & r > a \end{cases}$, $H_z = \begin{cases} BJ_l(hr)e^{j(l\phi-\beta z)}, & r \le a \\ DK_l(hr)e^{j(l\phi-\beta z)}, & r > a \end{cases}$

$$E_r = \begin{cases} \frac{-j\beta}{h^2}[AhJ_l'(hr) + \frac{j\omega\mu l}{\beta r}BJ_l(hr)]\cdot e^{j(l\phi-\beta z)}, & r \le a \\ \frac{j\beta}{q^2}[CqK_l'(qr) + \frac{j\omega\mu l}{\beta r}DK_l(qr)]\cdot e^{j(l\phi-\beta z)}, & r > a \end{cases}$$

$$E_\phi = \begin{cases} \frac{-j\beta}{h^2}[\frac{jl}{r}AJ_l(hr) - \frac{\omega\mu}{\beta}BhJ_l'(hr)]\cdot e^{j(l\phi-\beta z)}, & r \le a \\ \frac{j\beta}{q^2}[\frac{jl}{r}CK_l'(qr) - \frac{\omega\mu}{\beta}DqK_l(qr)]\cdot e^{j(l\phi-\beta z)}, & r > a \end{cases}$$

$$H_r = \begin{cases} \frac{-j\beta}{h^2}[BhJ_l'(hr) - \frac{j\omega\varepsilon_1 l}{\beta r}AJ_l(hr)]\cdot e^{j(l\phi-\beta z)}, & r \le a \\ \frac{j\beta}{q^2}[DqK_l'(qr) - \frac{j\omega\varepsilon_2 l}{\beta r}CK_l(qr)]\cdot e^{j(l\phi-\beta z)}, & r > a \end{cases}$$

$$H_\phi = \begin{cases} \frac{-j\beta}{h^2}[\frac{jl}{r}BJ_l(hr) + \frac{\omega\varepsilon_1}{\beta}AhJ_l'(hr)]\cdot e^{j(l\phi-\beta z)}, & r \le a \\ \frac{j\beta}{q^2}[\frac{jl}{r}DK_l(qr) + \frac{\omega\varepsilon_2}{\beta}CqK_l'(qr)]\cdot e^{j(l\phi-\beta z)}, & r > a \end{cases}$$

where $h = \sqrt{n_1^2 k_0^2 - \beta^2}$, $q = \sqrt{\beta^2 - n_2^2 k_0^2}$, l is an integer, and h is the m^{th} roots of

$$\left(\frac{J_l'(ha)}{haJ_l(ha)} + \frac{K_l'(qa)}{qaK_l(qa)}\right)\cdot\left(\frac{n_1^2 J_l'(ha)}{haJ_l(ha)} + \frac{n_2^2 K_l'(qa)}{qaK_l(qa)}\right) = [(\frac{1}{ha})^2 + (\frac{1}{qa})^2]\cdot(\frac{l\beta}{k_0})^2.$$

The constants A, B, C, and D satisfy the boundary conditions that the tangential field components are continuous at $r=a$. This leads to $AJ_l(ha) - CK_l(qa) = 0$,

$$A\cdot[\frac{jl}{h^2 a}J_l(ha)] + B\cdot[\frac{-\omega\mu}{h\beta}J_l'(ha)] + C\cdot[\frac{jl}{q^2 a}K_l(qa)] + D\cdot[\frac{-\omega\mu}{q\beta}K_l'(qa)] = 0,$$

$$A\cdot[\frac{\omega\varepsilon_1}{h\beta}J_l'(ha)] + B\cdot[\frac{jl}{h^2 a}J_l(ha)] + C\cdot[\frac{\omega\varepsilon_2}{q\beta}K_l'(qa)] + D\cdot[\frac{jl}{q^2 a}K_l(qa)] = 0.$$

Note: Other approximate solutions of the eigenmodes are called LP_{ij} modes. Their expressions are omitted in this course.

Single-mode operation of the step-index fiber: $\frac{2\pi a\cdot\sqrt{n_1^2 - n_2^2}}{\lambda_0} < 2.405$

Eg. A step-index fiber with n_1=1.45 and n_2=1.44, has a core radius a=2.5μm. Find the minimum free-space wavelength for single-mode operation.

(Sol.) $\dfrac{2\pi \cdot 2.5 \cdot \sqrt{1.45^2 - 1.44^2}}{\lambda_0} < 2.405, \quad \lambda_0 > 1.11033 \mu m$

***Case 2 Graded-index fiber*:** the core region has a parabolic refractive index profile $n_1^2(x,y)=n_1^2(r)= n_{10}^2(1-\alpha^2 r^2)= n_{10}^2[1-\alpha^2(x^2+y^2)]$

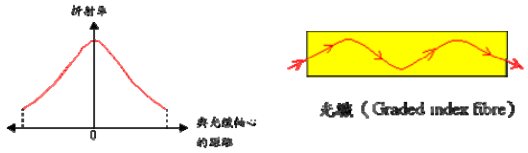

Ray tracing in the z-directional graded-index medium: Assume initial angle θ_0 from the vertical.

$$\text{Snell's law} \Rightarrow n_0 \sin\theta_0 = n_1 \sin\theta_1 = n_2 \sin\theta_2 = \cdots \Rightarrow \frac{dz}{dx} = \frac{n_0 \sin\theta_0}{\sqrt{n^2 - n_0^2 \sin^2\theta_0}}$$

Eg. For a medium with $n^2(x)=n_0^2(1-\alpha^2x^2)$, find the trajectory of a ray making an initial angle φ_0 with the z-axis in case of $\alpha^2x^2<<1$.

(Sol.) $\dfrac{dz}{dx} = \dfrac{n_0 \sin\theta_0}{\sqrt{n^2 - n_0^2 \sin^2\theta_0}} = \dfrac{\cos\phi_0}{\sqrt{\sin^2\phi_0 - \alpha^2 x^2}} \approx \dfrac{1}{[\phi_0^2 - \alpha^2 x^2]^{\frac{1}{2}}} \Rightarrow x = \dfrac{\phi_0 \sin(\alpha z)}{\alpha}$

WKB method: $\dfrac{4\pi}{\lambda_0}\int_0^{x_a} \sqrt{n^2(x) - n^2(x_a)}\,dx = (m+\frac{1}{2})\pi$, where x_a is the turning point of the m^{th}-order-mode ray.

For $n^2(x)=n_0^2(1-\alpha^2x^2)$, $\dfrac{4\pi}{\lambda_0}\int_0^{x_a} \sqrt{n^2(x) - n^2(x_a)}\,dx = \dfrac{4\pi n_0 \alpha}{\lambda_0}\int_0^{x_a} \sqrt{x_a^2 - x^2}\,dx = (m+\frac{1}{2})\pi$

$$\Rightarrow x_a^2 = \frac{(2m+1)\lambda_0}{2\pi n_0 \alpha} \quad \text{and} \quad x = x_a \sin(\alpha z) = \sqrt{\frac{(2m+1)\lambda_0}{2\pi n_0 \alpha}} \sin(\alpha z)$$

1.32μm and 1.55μm are commonly-used wavelengths for fiber communications.

Fiber Systems:

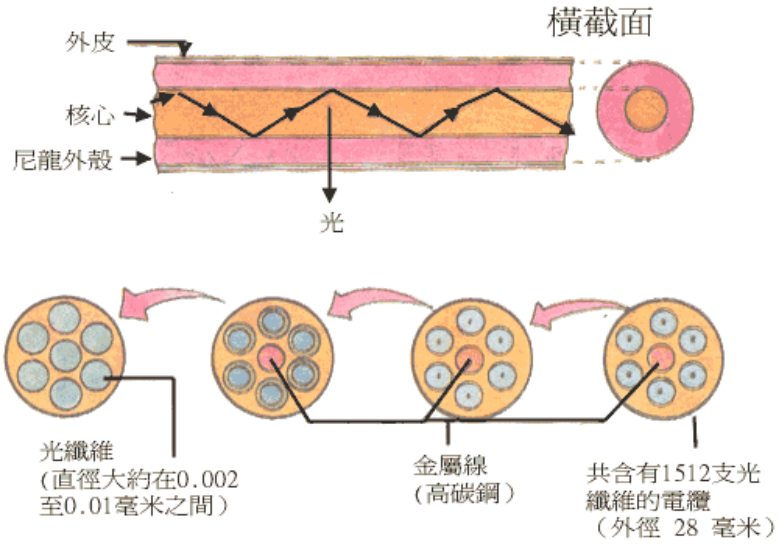

COMMUNICATION REQUIRES ENERGY AND POWER

Power Requirements

Typical receivers need: $E_b > \sim 4 \times 10^{-20}$ Joules/bit

Power received [W]: $P = M_{bps}E_b$ (M_{bps} is data rate, bits/sec)

e.g. 10^{-9} Watts permits $M_{bps} = \sim 10^{-9}/4 \times 10^{-20} = 2.5 \times 10^{10}$ bps

This can send $2.5 \times 10^{10}/(8 \times 7 \times 10^{8}$ bits/CD) = 4.5 CD's/second!)

WAVELENGTH DIVISION MULTIPLEXING (WDM):

- Multiple wavelengths combined onto one fiber
- All wavelengths amplified simultaneously and independently in each optical amplifier (OAMP)

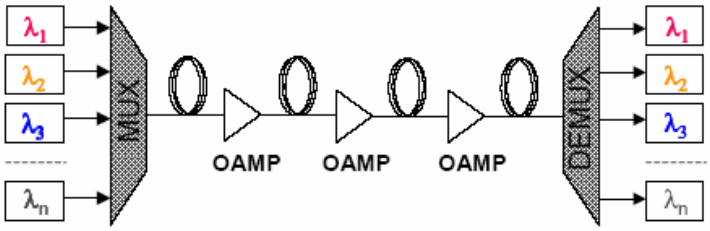

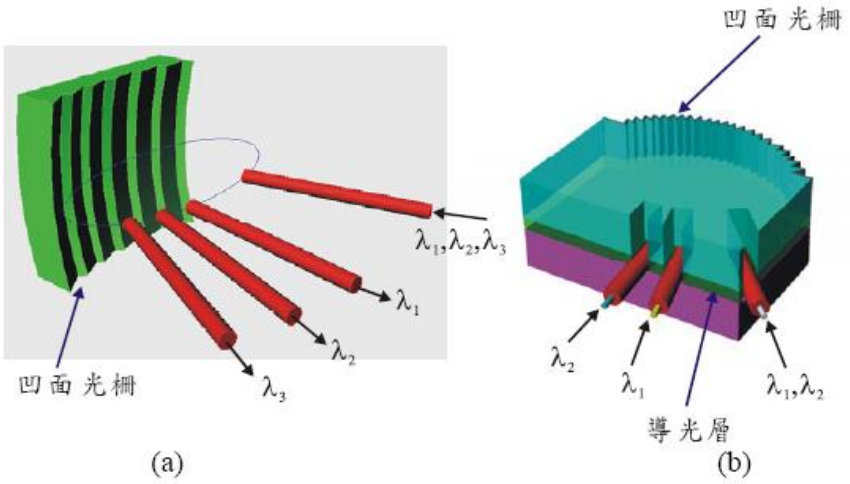

應用反射光柵實現分波解多工器示意圖（一）

(a)自由空間型中三維凹面光柵。(b)波導型二維凹面光柵

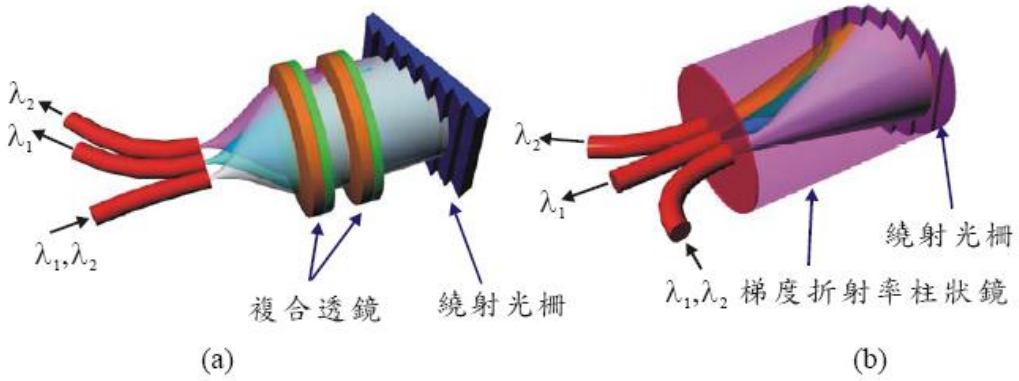

應用反射光柵實現分波解多工器示意圖（二）

(a) 自由空間型反射光柵系統。(b) 梯度折射率柱狀透鏡型反射光柵系統。

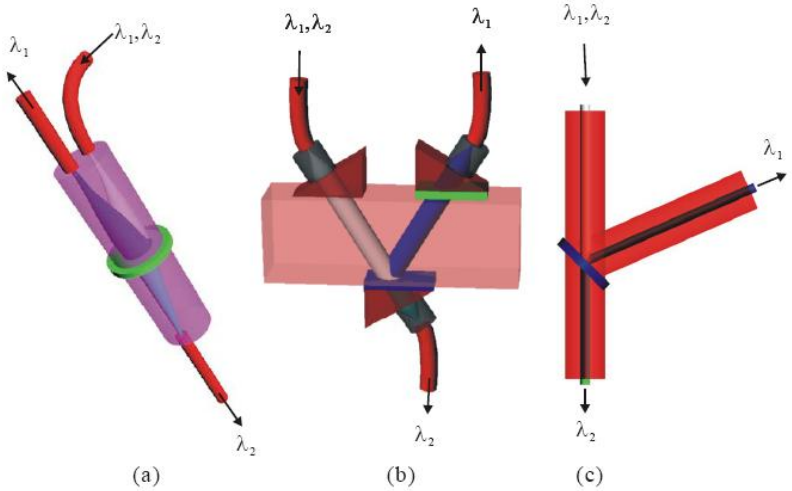

應用薄膜濾波器實現分波解多工器示意圖。

(a)梯度折射率柱狀透鏡型。(b)多重反射型。(c)光纖端點濾波型

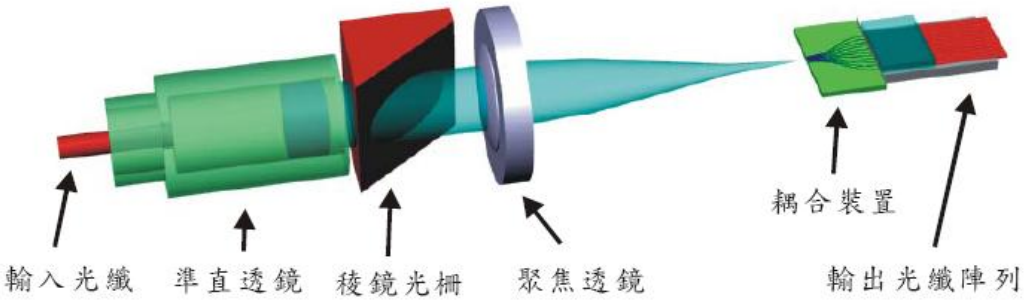

應用稜鏡光柵結構實現分波解多工系統的示意圖

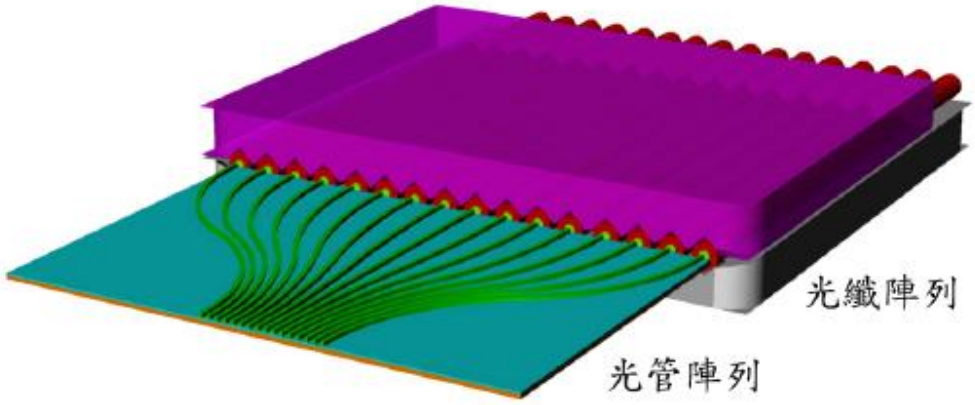

光管陣列與光纖陣列的接合情形

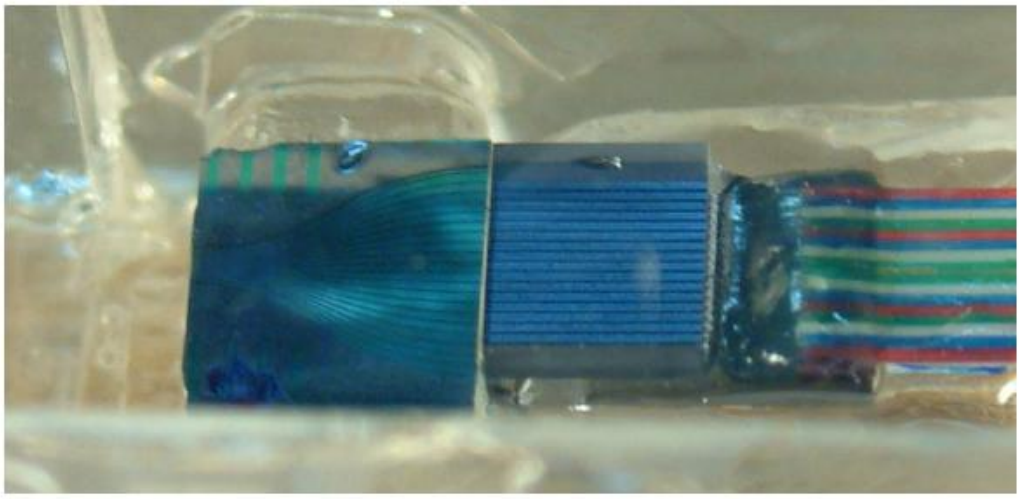

光管陣列與商用光纖陣列的接合情形

A 16-wavelength DWDM fiber system (by Dr. J. -R. Sze, 施至柔博士):

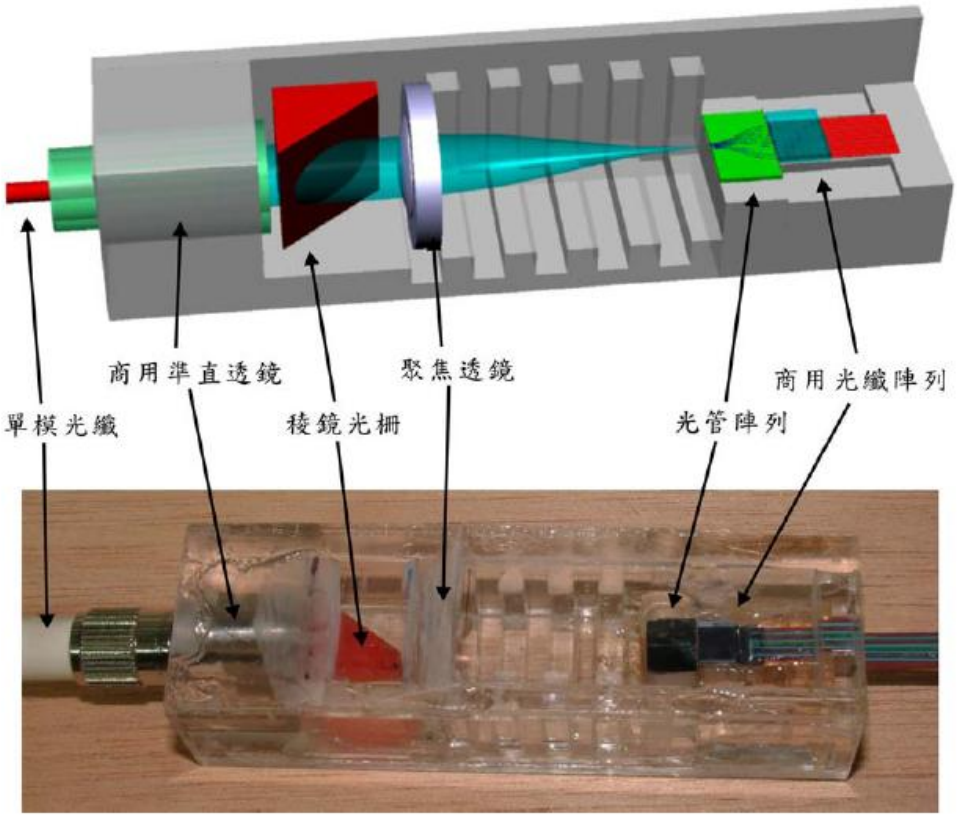

分波解多工系統的封裝結果

封裝後十六通道的分波解多工系統實體照片

7-5 Planar Optical Waveguides

Consider a *z*-directional planar (slab) waveguide with the refractive index profile $n(x)=\begin{cases} n_c, & x \ge d \\ n_f, & |x| \le d \\ n_s, & x \le -d \end{cases}$, its eigenmodes are

***Case 1 TE modes*:** $\vec{E} = \hat{y}E_y(x)$

$$E_y(x) = \begin{cases} E_0 e^{-q(x-d)}, & x \ge d \\ E_0\{\cos[h(x-d)] - \frac{q}{h}\sin[h(x-d)]\}, & |x| \le d \\ E_0\{\cos(2hd) + \frac{q}{h}\sin(2hd)]\} \cdot e^{p(x+d)}, & x \le -d \end{cases}$$, where $q = \sqrt{\beta^2 - {n_c}^2 k^2}$,

$p = \sqrt{\beta^2 - {n_s}^2 k^2}$, $h = \sqrt{{n_f}^2 k^2 - \beta^2}$, and $\tan(2hd) = \dfrac{p+q}{h - \dfrac{pq}{h}}$ $\Rightarrow$ Solve β=?

***Case 2 TM modes*:** $\vec{H} = \hat{y}H_y(x)$

$$H_y(x) = \begin{cases} -H_0 \frac{h}{q'} e^{-q'(x-d)}, & x \ge d \\ H_0\{-\frac{h}{q'}\cos[h(x-d)] + \sin[h(x-d)]\}, & |x| \le d \\ -H_0[\frac{h}{q'}\cos(2hd) + \sin(2hd)] \cdot e^{p'(x+d)}, & x \le -d \end{cases}$$, where $q' = \dfrac{{n_f}^2}{{n_s}^2} \cdot q$, $p' = \dfrac{{n_f}^2}{{n_c}^2} \cdot p$,

and $\tan(2hd) = \dfrac{p'+q'}{h - \dfrac{p'q'}{h}}$ $\Rightarrow$ Solve β=?

Condition of single-mode waveguide: β has exactly only one value.

Eg. Let $n_c=n_s=n_0$, the ray paths and optical field distributions are depicted as follows:

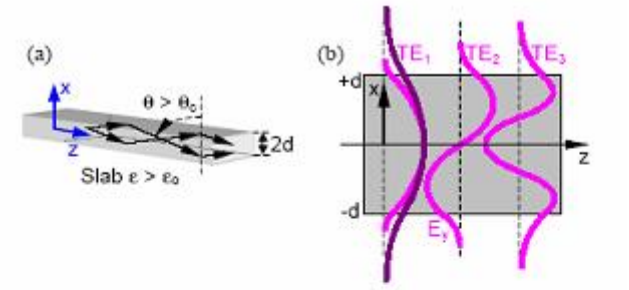

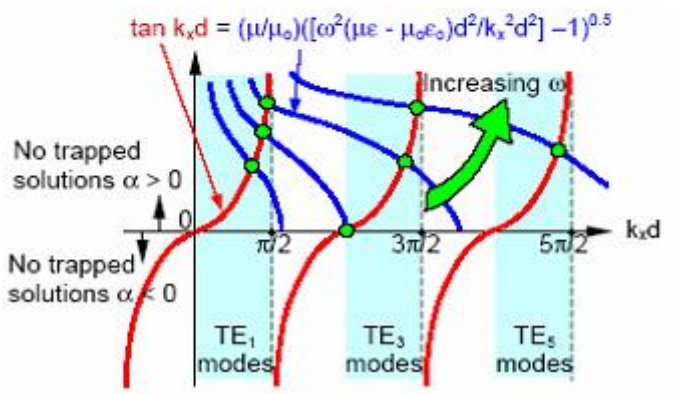

$$\begin{cases} \beta^2 + k_x^{\ 2} = \omega^2 \mu\varepsilon, & inside\ the\ slab \\ \beta^2 - \alpha^2 = \omega^2 \mu_0 \varepsilon_0, & outside\ the\ slab \end{cases} \Rightarrow k_x^{\ 2} + \alpha^2 = \omega^2(\mu\varepsilon - \mu_0\varepsilon_0)$$

Transcendental equation: $k_x d \tan(k_x d) = \mu d\sqrt{\omega^2(\mu\varepsilon - \mu_0\varepsilon_0) - k_x^{\ 2}} \,/\, \mu_0$

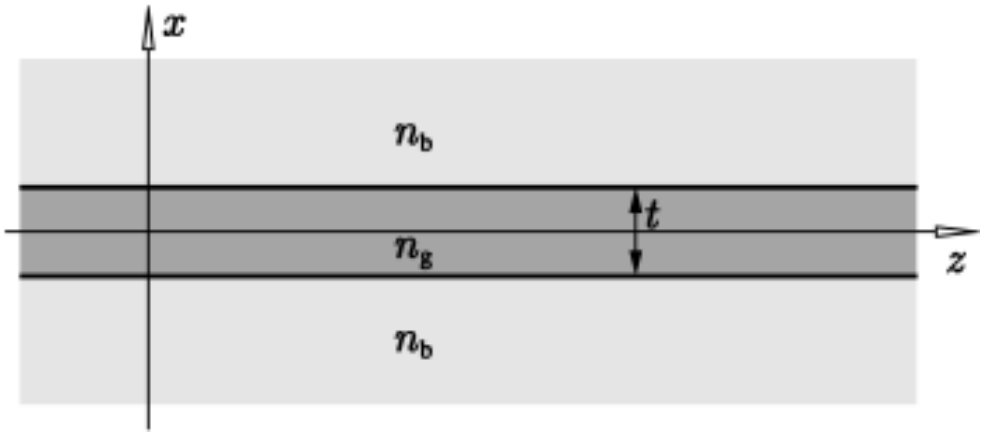

Eg. Determine β for an optical planar waveguide with $2d=t=1\mu m$ and $n_c=n_s=1.49=n_b$, $n_f=1.5=n_g$ by numerical methods. Is it single-mode? And sketch the *E*-field profile. (Assume $\lambda=1\mu m$.)

7-6 Rectangular Optical Waveguides Surrounding by a Uniform Medium

Consider a *z*-directional rectangular optical waveguide surrounding by a uniform material with the refractive index distribution $n(x,y)=\begin{cases} n_1, & |x|\le a,\ |y|\le d \\ n_2, & elsewhere \end{cases}$. Its eigenmodes cannot be solved by analytic methods. Therefore, some approximate methods were proposed.

Marcatili's approximation:

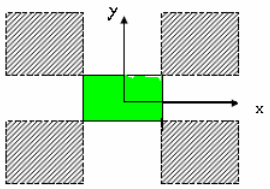

Divide the transverse section into nine regions. The fields within the four corner regions are neglected and the sinusoidal-sinusoidal field exists within the core region. The sinusoidal-exponential fields exist within the upper, lower, left, and right regions. According to Marcatili's theory, a rectangular waveguide supports E_{pq}^{x} and E_{pq}^{y} modes.

Case 1 E_{pq}^{x} **mode (*p* and *q* are integers):** $H_x=0$

$$H_y=\begin{cases} A\cos(k_x x-\phi)\cos(k_y y-\psi), & |x|\le a, |y|\le d \\ A\cos(k_x a-\phi)\cos(k_y y-\psi)e^{-\gamma_x(x-a)}, & x>a, |y|\le d \\ A\cos(k_x x-\phi)\cos(k_y d-\psi)e^{-\gamma_y(y-d)}, & |x|\le a, y>d \\ A\cos(-k_x a-\phi)\cos(k_y y-\psi)e^{\gamma_x(x+a)}, & x<-a, |y|\le d \\ A\cos(k_x x-\phi)\cos(-k_y d-\psi)e^{\gamma_y(y+d)}, & |x|\le a, y<-d \end{cases}$$

where phase parameters $\phi=(p-1)\pi/2$, $\psi=(q-1)\pi/2$,

and $\begin{cases} k_x^2+k_y^2+\beta^2=k^2n_1^2, & |x|\le a,\ |y|\le d \\ -\gamma_x^2+k_y^2+\beta^2=k^2n_2^2, & x>a\ or\ x<-a,\ |y|\le d \\ k_x^2-\gamma_y^2+\beta^2=k^2n_2^2, & |x|\le a,\ y>d\ or\ y<-d \end{cases}$. Transverse wavenumbers are $\gamma_x^2=k^2(n_1^2-n_2^2)-k_x^2$ and $\gamma_y^2=k^2(n_1^2-n_2^2)-k_y^2$.

The other field components can be obtained by

$$\begin{cases} E_x=\dfrac{\omega\mu_0}{\beta}H_y+\dfrac{1}{\omega\varepsilon_0 n^2\beta}\dfrac{\partial^2 H_y}{\partial x^2}, & E_y=\dfrac{1}{\omega\varepsilon_0 n^2\beta}\dfrac{\partial^2 H_y}{\partial x\partial y} \\ E_z=\dfrac{-j}{\omega\varepsilon_0 n^2}\dfrac{\partial H_y}{\partial x}, & H_z=\dfrac{-j}{\beta}\dfrac{\partial H_y}{\partial y} \end{cases}$$

E_z and H_z are continuous at $x=\pm a$ and $y=\pm d$

$$\Rightarrow k_x a = (p-1)\frac{\pi}{2} + \tan^{-1}\left(\frac{n_1^2 \gamma_x}{n_2^2 k_x}\right) \quad \text{and} \quad k_y d = (q-1)\frac{\pi}{2} + \tan^{-1}\left(\frac{\gamma_y}{k_y}\right)$$

Case 2 E_{pq}^{y} **mode:** $H_y=0$

$$H_x = \begin{cases} B\cos(k_x x-\phi)\cos(k_y y-\psi), & |x|\le a, |y|\le d \\ B\cos(k_x a-\phi)\cos(k_y y-\psi)e^{-\gamma_x(x-a)}, & x>a, |y|\le d \\ B\cos(k_x x-\phi)\cos(k_y d-\psi)e^{-\gamma_y(y-d)}, & |x|\le a, y>d \\ B\cos(-k_x a-\phi)\cos(k_y y-\psi)e^{\gamma_x(x+a)}, & x<-a, |y|\le d \\ B\cos(k_x x-\phi)\cos(-k_y d-\psi)e^{\gamma_y(y+d)}, & |x|\le a, y<-d \end{cases}$$

The other field components:

$$\begin{cases} E_y = -\dfrac{\omega\mu_0}{\beta}H_x - \dfrac{1}{\omega\varepsilon_0 n^2\beta}\dfrac{\partial^2 H_x}{\partial y^2}, & E_x = -\dfrac{1}{\omega\varepsilon_0 n^2\beta}\dfrac{\partial^2 H_x}{\partial x\partial y} \\ E_z = \dfrac{j}{\omega\varepsilon_0 n^2}\dfrac{\partial H_x}{\partial x}, & H_z = \dfrac{-j}{\beta}\dfrac{\partial H_x}{\partial y} \end{cases}$$

E_z and H_z are continuous at $x=\pm a$ and $y=\pm d$

$$\Rightarrow k_x a = (p-1)\frac{\pi}{2} + \tan^{-1}\left(\frac{\gamma_x}{k_x}\right) \quad \text{and} \quad k_y d = (q-1)\frac{\pi}{2} + \tan^{-1}\left(\frac{n_1^2 \gamma_y}{n_2^2 k_y}\right)$$

Examples of rectangular waveguides (by Dr. J. -R. Sze, 施至柔博士)—Light pipe (multimode rectangular ridge waveguide) array.

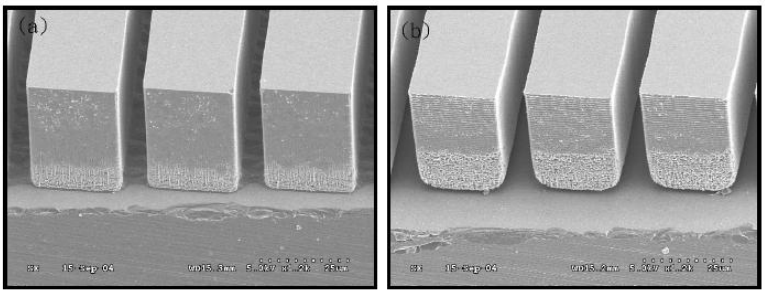

製作完成的局部光管陣列電子掃描顯微鏡照片（一）。
(a)鏡面蝕刻。(b)一般蝕刻。

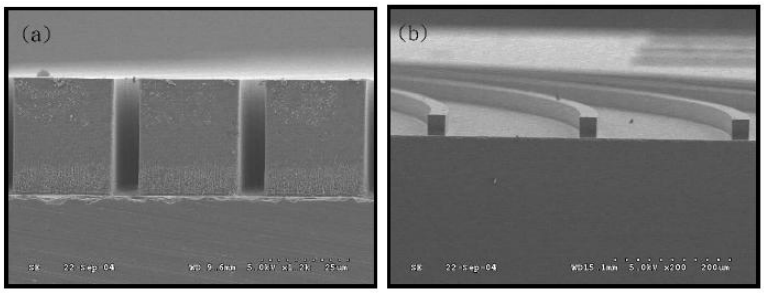

製作完成的光管陣列局部電子掃描顯微鏡照片（二）。
(a)輸入端。(b)輸出端。

Helmholtz's equation: $\nabla_t^2\phi(x,y)+[k^2n^2(x,y)-\beta^2]\phi(x,y)=0$, **where $\varphi(x,y)$ is the scalar field.**

(Proof) Scalar wave equation: $\nabla^2\Psi(x,y,z)+k^2n^2(x,y,z)\Psi(x,y,z)=0$

For a z-directional waveguide: $n(x,y,z)=n(x,y)$. Let $\Psi(x,y,z)=\phi(x,y)e^{-j\beta z}$, we obtain $\nabla_t^2\phi(x,y)+[k^2n^2(x,y)-\beta^2]\phi(x,y)=0$

Variational principle: Seek a trial function $\varphi(x,y)$ to maximize

$$\beta^2=\frac{\int_{-\infty}^{\infty}\int_{-\infty}^{\infty}[k^2n^2(x,y)|\phi(x,y)|^2-|\nabla_t\phi(x,y)|^2]dxdy}{\int_{-\infty}^{\infty}\int_{-\infty}^{\infty}|\phi(x,y)|^2dxdy}$$

(Proof)

$$\nabla_t^2\phi(x,y)+[k^2n^2(x,y)-\beta^2]\phi(x,y)=0$$

$$\nabla_t^2\phi(x,y)+k^2n^2(x,y)\phi(x,y)=\beta^2\phi(x,y)$$

$$\phi^*(x,y)\nabla_t^2\phi(x,y)+k^2n^2(x,y)\phi(x,y)\phi^*(x,y)=\beta^2\phi(x,y)\phi^*(x,y)$$

$$\int_{-\infty}^{\infty}\int_{-\infty}^{\infty}[\phi^*(x,y)\nabla_t^2\phi(x,y)+k^2n^2(x,y)|\phi(x,y)|^2]dxdy=\beta^2\int_{-\infty}^{\infty}\int_{-\infty}^{\infty}|\phi(x,y)|^2dxdy$$

For $\phi(x\to\pm\infty,y\to\pm\infty)=0$, $\int_{-\infty}^{\infty}\int_{-\infty}^{\infty}\phi^*(x,y)\nabla_t^2\phi(x,y)dxdy=-\int_{-\infty}^{\infty}\int_{-\infty}^{\infty}|\nabla_t\phi(x,y)|^2dxdy$

$$\Rightarrow\beta^2=\frac{\int_{-\infty}^{\infty}\int_{-\infty}^{\infty}[k^2n^2(x,y)|\phi(x,y)|^2-|\nabla_t\phi(x,y)|^2]dxdy}{\int_{-\infty}^{\infty}\int_{-\infty}^{\infty}|\phi(x,y)|^2dxdy}$$

Utilizing the variational principle, two common trial modal functions for a rectangular optical waveguide are

$$\phi_1(x,y)=\sqrt{\frac{2}{w_xw_y\pi}}\cdot\exp(-\frac{x^2}{w_x^2}-\frac{y^2}{w_y^2})\quad\text{and}\quad\phi_2(x,y)=\sqrt[4]{\frac{4(e-1)}{\alpha^2\gamma^2\pi^3}}\cdot\frac{\exp(-\frac{x^2}{\alpha^2})}{1+(e-1)\cdot y^2/\gamma^2}$$

Some simulation results of a multimode rectangular optical waveguide are depicted as follows:

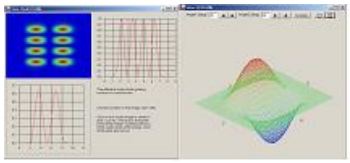

7-7 Diffused Waveguides

Waveguides were fabricated by diffusing a strip of metal, width W, into a chip. Let the y-axis be downward, and the origin is set on the surface of the chip, then the refractive index profile becomes $n^2(x,y)=\begin{cases} 1, & y<0 \\ n_b^{\,2}+(n_s^{\,2}-n_b^{\,2})f(y)g(x), & y\geq 0 \end{cases}$, where

$$f(y)=\exp(-\frac{y^2}{D_y^{\,2}}),\quad g(x)=\frac{1}{2}\{erf[\frac{W(1+2x/W)}{2D_x}]+erf[\frac{W(1-2x/W)}{2D_x}]\},$$

n_b is the refractive index of the bulk, and n_s is the refractive index on the surface for a sufficient wide metal strip. The quantities D_x and D_y are respectively the diffusion width and depth.

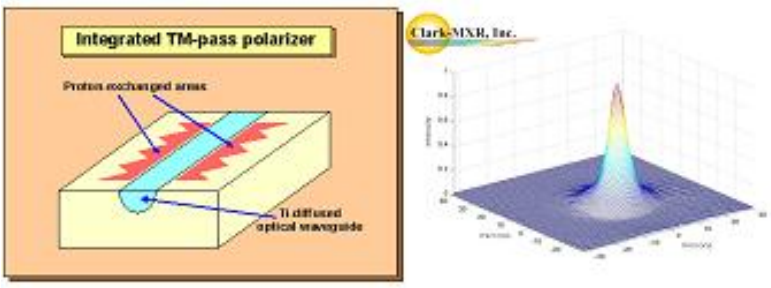

The approximate fundamental modal functions of diffused waveguide is normalized as

$$\phi(x,y)=\sqrt{\frac{4}{a_1(a_2+a_3)\pi}}\cdot\exp[-\frac{x^2}{a_1^{\,2}}-\frac{(y-b)^2}{a_i^{\,2}}],\quad i=\begin{cases}2, & y<b\\ 3, & y\geq b\end{cases}$$

where a_1 is the horizontal e^{-1} half width of the modal field. Both parameters a_2 and a_3 are the vertical e^{-1} half widths toward the air and the substrate, respectively. The other parameter b denotes the distance between the peak of the modal field and the top surface of the core region.

For a general 3D optical waveguide, its waveguiding modes and propagating field can be solved by **BPM** in case of ignoring reflection. If the structure is very complicated, **FDTD** method is employed.

7-8 Introductions to Finite-difference Beam Propagation Method (FDBPM)

Consider a source-free region and set $\vec{E} = \hat{x}E'_x + \hat{y}E'_y + \hat{z}E'_z$.

E-formulation (by Dr. Wei-Ping Huang):

Dr. Wei-Ping Huang was born in Beijing. He graduated from MIT and got his PhD degree. Now he is a professor in the ECE Department at the University of Waterloo, Canada. His research group is one of the leading groups internationally in photonics and computer aided design. Dr. Huang is creating new design tools to help develop the cost-efficient photonics systems required for large-scale broadband communication.

血染的風采(原為 1979 年中共出兵教訓越南時所作之軍歌，後為 1989 年北京「六四事件」天安門廣場學生主題歌，而被中共禁唱很長一段時間)

也許我告別 將不再回來 你是否理解 你是否明白
也許我倒下 將不再起來 你是否還要 永久的期待
如果是這樣 你不要悲哀 共和國的旗幟上有我們血染的風采
也許我的眼睛 再不能睜開 你是否理解 我沉默的情懷
也許我長眠 再不能醒來 你是否相信 我化作了山脈
如果是這樣 你不要悲哀 共和國的土壤裏有我們付出的愛

$$\nabla\times\nabla\times\vec{E} - n^2k^2\vec{E} = \nabla(\nabla\cdot\vec{E}) - \nabla^2\vec{E} - n^2k^2\vec{E} = 0 \Rightarrow \nabla^2\vec{E} + n^2k^2\vec{E} = \nabla(\nabla\cdot\vec{E})$$

$$\Rightarrow \nabla^2(\hat{x}E'_x + \hat{y}E'_y + \hat{z}E'_z) + n^2k^2(\hat{x}E'_x + \hat{y}E'_y + \hat{z}E'_z) = \nabla\left(\frac{\partial E'_x}{\partial x} + \frac{\partial E'_y}{\partial y} + \frac{\partial E'_z}{\partial z}\right)$$

$\because$ No source, $\therefore \nabla\cdot(\varepsilon\vec{E}) = \nabla\cdot(n^2\vec{E}) = 0 \Rightarrow \dfrac{\partial(n^2E'_x)}{\partial x} + \dfrac{\partial(n^2E'_y)}{\partial y} + \dfrac{\partial n^2}{\partial z}E'_z + n^2\dfrac{\partial E'_z}{\partial z} = 0$

If the refractive index profile varies slowly along the z-axis, $\partial n^2/\partial z$ may be neglected. $\Rightarrow \dfrac{\partial E'_z}{\partial z} \approx -\dfrac{1}{n^2}\left[\dfrac{\partial(n^2E'_x)}{\partial x} + \dfrac{\partial(n^2E'_y)}{\partial y}\right]$

$$\nabla^2(\hat{x}E'_x + \hat{y}E'_y + \hat{z}E'_z) + n^2k^2(\hat{x}E'_x + \hat{y}E'_y + \hat{z}E'_z)$$

$$= \left(\hat{x}\frac{\partial}{\partial x} + \hat{y}\frac{\partial}{\partial y} + \hat{z}\frac{\partial}{\partial z}\right)\left(\frac{\partial E'_x}{\partial x} + \frac{\partial E'_y}{\partial y} - \frac{1}{n^2}\left[\frac{\partial(n^2E'_x)}{\partial x} + \frac{\partial(n^2E'_y)}{\partial y}\right]\right)$$

$$\Rightarrow \nabla^2E'_x + n^2k^2E'_x = \frac{\partial}{\partial x}\left\{\frac{\partial E'_x}{\partial x} + \frac{\partial E'_y}{\partial y} - \frac{1}{n^2}\left[\frac{\partial(n^2E'_x)}{\partial x} + \frac{\partial(n^2E'_y)}{\partial y}\right]\right\},$$

and $\nabla^2E'_y + n^2k^2E'_y = \dfrac{\partial}{\partial y}\left\{\dfrac{\partial E'_x}{\partial x} + \dfrac{\partial E'_y}{\partial y} - \dfrac{1}{n^2}\left[\dfrac{\partial(n^2E'_x)}{\partial x} + \dfrac{\partial(n^2E'_y)}{\partial y}\right]\right\}$.

Assume that $E'_x = E_x e^{-jn_0 kz}$ and $E'_y = E_y e^{-jn_0 kz}$, where k is the vacuum wave number and n_0 is the effective refractive index. With the assumption that the guided lightwave has a slow-varying envelop and is paraxially propagating; i.e., $\left|\frac{\partial^2 E_x}{\partial z^2}\right| << 2n_0 k\left|\frac{\partial E_x}{\partial z}\right|$, $\left|\frac{\partial^2 E_y}{\partial z^2}\right| << 2n_0 k\left|\frac{\partial E_y}{\partial z}\right| \Rightarrow \left|\frac{\partial^2 E_x}{\partial z^2}\right|$ and $\left|\frac{\partial^2 E_y}{\partial z^2}\right|$ are neglected.

And then we have the following coupled equations

$$\begin{cases} j\dfrac{\partial E_x}{\partial z} = A_{xx}E_x + A_{xy}E_y \\ j\dfrac{\partial E_y}{\partial z} = A_{yy}E_y + A_{yx}E_x \end{cases}$$

where

$$\begin{cases} A_{xx}E_x = \dfrac{1}{2n_0 k}\left\{\dfrac{\partial}{\partial x}\left[\dfrac{1}{n^2}\dfrac{\partial}{\partial x}\left(n^2 E_x\right)\right] + \dfrac{\partial^2}{\partial y^2}E_x + \left(n^2 - {n_0}^2\right)\cdot k^2 E_x\right\} \\ A_{yy}E_y = \dfrac{1}{2n_0 k}\left\{\dfrac{\partial^2}{\partial x^2}E_y + \dfrac{\partial}{\partial y}\left[\dfrac{1}{n^2}\dfrac{\partial}{\partial y}\left(n^2 E_y\right)\right] + \left(n^2 - {n_0}^2\right)\cdot k^2 E_y\right\} \\ A_{xy}E_y = \dfrac{1}{2n_0 k}\left\{\dfrac{\partial}{\partial x}\left[\dfrac{1}{n^2}\dfrac{\partial}{\partial y}\left(n^2 E_y\right)\right] - \dfrac{\partial^2}{\partial x \partial y}E_y\right\} \\ A_{yx}E_x = \dfrac{1}{2n_0 k}\left\{\dfrac{\partial}{\partial y}\left[\dfrac{1}{n^2}\dfrac{\partial}{\partial x}\left(n^2 E_x\right)\right] - \dfrac{\partial^2}{\partial y \partial x}E_x\right\} \end{cases}$$

These coupled equations are the basic formulas of the full-vector BPM. If we neglect the terms of A_{xy} and A_{yx}, then the equations are reduced to the formulas of the semi-vector BPM. In case the transverse variation of the refractive index is very small, and that is, $\frac{1}{n^2}\frac{\partial}{\partial x}(n^2 E_x) \approx \frac{\partial E_x}{\partial x}$ and $\frac{1}{n^2}\frac{\partial}{\partial y}(n^2 E_y) \approx \frac{\partial E_y}{\partial y}$.

The formulas of the semi-vector BPM can be simplified into the following Fresnel equation, which is the formula of the scalar BPM.

黃金剩女

Application of BPM:

Eg. A laser beam passes an MMI waveguide device. (by K. Huang, 黃建智)

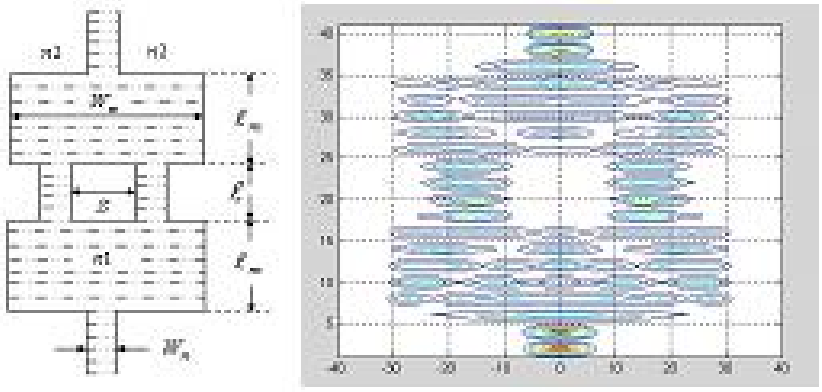

Eg. The fundamental modal field of a single-mode ridge waveguide.

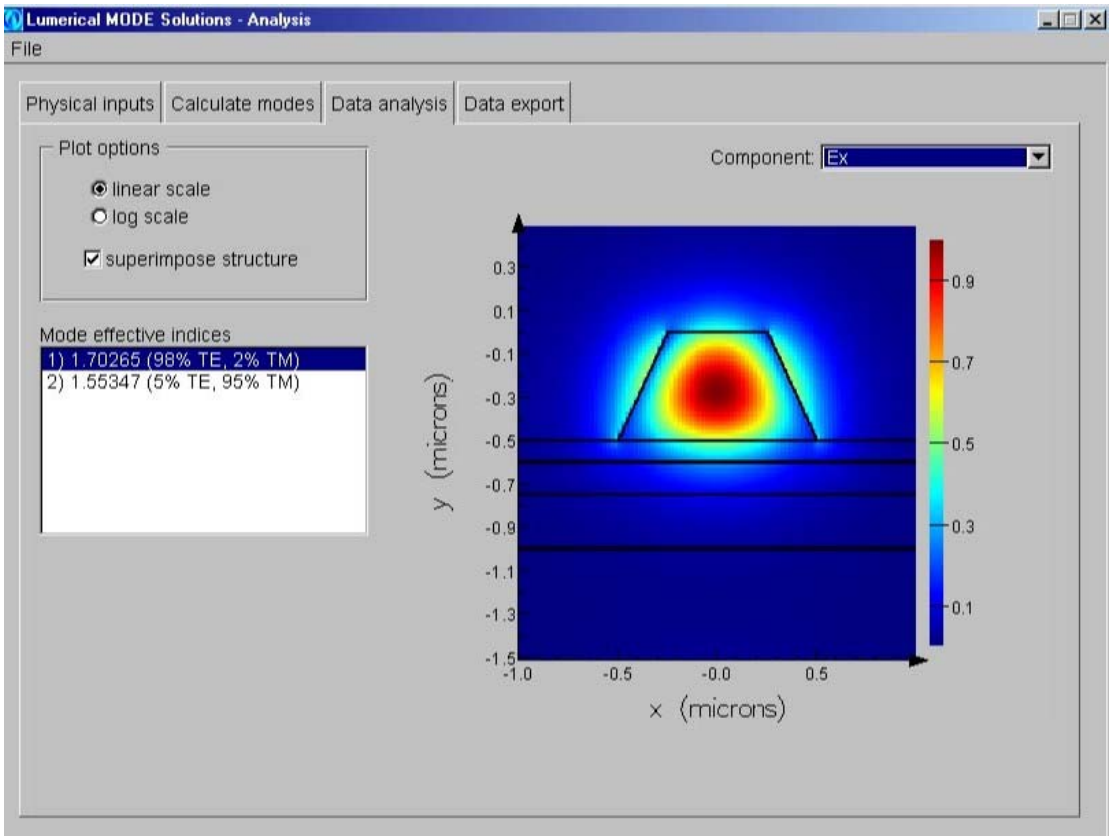

7-9 Direct Coupling from Laser-to-Waveguide

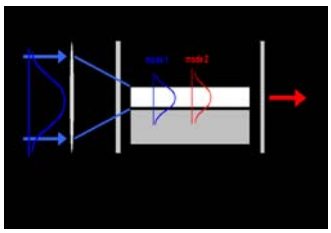

Direct coupling efficiency:

$$\eta = \frac{\left|\int_{-\infty}^{\infty}\int_{-\infty}^{\infty}\phi(x,y)\varphi^{*}(x,y)dxdy\right|^{2}}{\int_{-\infty}^{\infty}\int_{-\infty}^{\infty}\left|\phi(x,y)\right|^{2}dxdy\cdot\int_{-\infty}^{\infty}\int_{-\infty}^{\infty}\left|\varphi(x,y)\right|^{2}dxdy}$$

Optimal Direct Coupling from Single-Mode Fibers to Ti:$LiNbO_3$ Channel Waveguides

KEH-YI LEE
CHYI-JIEH HSIEH
JYH-ROU SZE
GWO-JIUNN JAW

Department of Electrical Engineering
Chinese Culture University
Taipei Taiwan, Republic of China

We investigate the optimal direct coupling from single-mode fibers to Ti:$LiNbO_3$ channel waveguides using a very general formula and a heuristic optimization technique in this article. The coupling efficiency of the optical power depends on both the fiber positions and the modal sizes of the incident fields. From our numerical simulation, it is found that the optimal positions of the fiber axes are not in alignment with the peaks of the waveguiding modal fields and that the coupling efficiency can be improved by microlenses.

Keywords coupling efficiency, optimization

Eg. Obtain the optimal direct coupling efficiency between an optical fiber and a diffused waveguide. (by K. –Y. Lee, J. –R. Sze, *et al.*)

(Sol.) Waveguide mode: $\varphi(x,y) = C_w \cdot \varphi_x(x)\varphi_y(y)$, where $\varphi_x(x) = \exp\left(-x^2/a_1^2\right)$

and $\varphi_y(y) = \exp\left[-(y-b)^2/a_i^2\right]$, $i = \begin{cases} 2, & y \le b \\ 3, & y > b \end{cases}$.

Fiber mode: $\phi(x,y) = C_f \cdot \exp\left\{-\left[x^2 + (y-c)^2\right]/w^2\right\}$

Utilize the following formulae: $\int_0^A e^{-t^2}dt = \frac{\sqrt{\pi}}{2}erf(A)$, $erf(-\infty) = -1$, $erf(0) = 0$,

$erf(\infty) = 1$, $erf(-C) = -erf(C)$, $\int_0^A e^{-Bt^2}dt = \frac{\sqrt{\pi}}{2\sqrt{B}}erf(A\sqrt{B})$, $\int_{-\infty}^{\infty} e^{-a^2x^2}dx = \frac{\sqrt{\pi}}{a}$,

$\int_{-\infty}^{A} e^{-t^2}\,dt = \frac{\sqrt{\pi}}{2}[1+erf(A)]$, $\int_{-\infty}^{0} e^{-(t-A)^2}\,dt = \frac{\sqrt{\pi}}{2}[1-erf(A)]$, and

$\int_{0}^{\infty} e^{-(t-A)^2}\,dt = \frac{\sqrt{\pi}}{2}[1+erf(A)]$

$\int_{-\infty}^{\infty}\int_{-\infty}^{\infty} \phi(x,y)\varphi(x,y)dxdy = C_f C_w \int_{-\infty}^{\infty} e^{-(\frac{1}{w^2}+\frac{1}{a_1^{\,2}})x^2}\,dx \cdot [\int_{-\infty}^{b} e^{-\frac{(y-c)^2}{w^2}-\frac{(y-b)^2}{a_2^{\,2}}}\,dy + \int_{b}^{\infty} e^{-\frac{(y-c)^2}{w^2}-\frac{(y-b)^2}{a_3^{\,2}}}\,dy]$

$\int_{-\infty}^{\infty} e^{-(\frac{1}{w^2}+\frac{1}{a_1^{\,2}})x^2}\,dx = \frac{wa_1\sqrt{\pi}}{\sqrt{w^2+a_1^{\,2}}}$,

$\int_{-\infty}^{b} e^{-\frac{(y-c)^2}{w^2}-\frac{(y-b)^2}{a_2^{\,2}}}\,dy = \int_{-\infty}^{0} e^{-\frac{[u-(c-b)]^2}{w^2}-\frac{u^2}{a_2^{\,2}}}\,du = e^{-\frac{(c-b)^2}{(a_2^{\,2}+w^2)}} \cdot \int_{-\infty}^{0} e^{-\frac{a_2^{\,2}+w^2}{w^2 a_2^{\,2}}\cdot[u-\frac{a_2^{\,2}(c-b)}{a_2^{\,2}+w^2}]^2}\,du$

$= \frac{a_2 w\sqrt{\pi}}{2\cdot\sqrt{a_2^2+w^2}} \cdot \exp\left[-\frac{(c-b)^2}{(a_2^2+w^2)}\right] \cdot \left\{1-erf\left[\frac{a_2(c-b)}{w\cdot\sqrt{a_2^{\,2}+w^2}}\right]\right\}$,

Similarly,

$\int_{b}^{\infty} e^{-\frac{(y-c)^2}{w^2}-\frac{(y-b)^2}{a_3^{\,2}}}\,dy = \int_{0}^{\infty} e^{-\frac{[u-(c-b)]^2}{w^2}-\frac{u^2}{a_3^{\,2}}}\,du = e^{-\frac{(c-b)^2}{(a_3^{\,2}+w^2)}} \cdot \int_{0}^{\infty} e^{-\frac{a_3^{\,2}+w^2}{w^2 a_3^{\,2}}\cdot[u-\frac{a_3^{\,2}(c-b)}{a_3^{\,2}+w^2}]^2}\,du$

$= \frac{a_3 w\sqrt{\pi}}{2\cdot\sqrt{a_3^2+w^2}} \cdot \exp\left[-\frac{(c-b)^2}{(a_3^2+w^2)}\right] \cdot \left\{1+erf\left[\frac{a_3(c-b)}{w\cdot\sqrt{a_3^{\,2}+w^2}}\right]\right\}$

$\int_{-\infty}^{\infty}\int_{-\infty}^{\infty} \phi^2(x,y)dxdy = C_f^{\,2}\cdot\frac{w^2\pi}{2}$, and $\int_{-\infty}^{\infty}\int_{-\infty}^{\infty} \varphi^2(x,y)dxdy = C_w^{\,2}\cdot\frac{a_1(a_2+a_3)\pi}{4}$,

$\Rightarrow \eta = \frac{2a_1 w^2}{(a_2+a_3)(a_1^2+w^2)}\cdot(I_1+I_2)^2$, where

$I_1 = \frac{a_2}{\sqrt{a_2^2+w^2}} \cdot \exp\left[-\frac{(c-b)^2}{(a_2^2+w^2)}\right] \cdot \left\{1-erf\left[\frac{a_2(c-b)}{w\cdot\sqrt{a_2^{\,2}+w^2}}\right]\right\}$

$I_2 = \frac{a_3}{\sqrt{a_3^2+w^2}} \cdot \exp\left[-\frac{(c-b)^2}{(a_3^2+w^2)}\right] \cdot \left\{1+erf\left[\frac{a_3(c-b)}{w\cdot\sqrt{a_3^{\,2}+w^2}}\right]\right\}$

Simulation:

λ = 1.32 μm		a_1	a_2	a_3	b	w	c	c − b	η
waveuide I made of 6 μm-wide 520 Å-thick Ti strip	quasi-TE (mode I)	5.10	2.10	4.60	3.10	4.15	4.20	1.10	0.942
	quasi-TM (mode II)	5.00	2.10	5.00	3.00	4.23	4.26	1.26	0.953
waveuide II made of 6 μm-wide 660 Å-thick Ti strip	quasi-TE (mode III)	4.60	2.10	3.80	2.80	3.69	3.55	0.75	0.944
	quasi-TM (mode IV)	3.50	2.10	2.10	2.00	2.71	1.99	0.01	0.937

a_1, a_2, a_3, b, w, c, and c − b : μm η : dimensionless

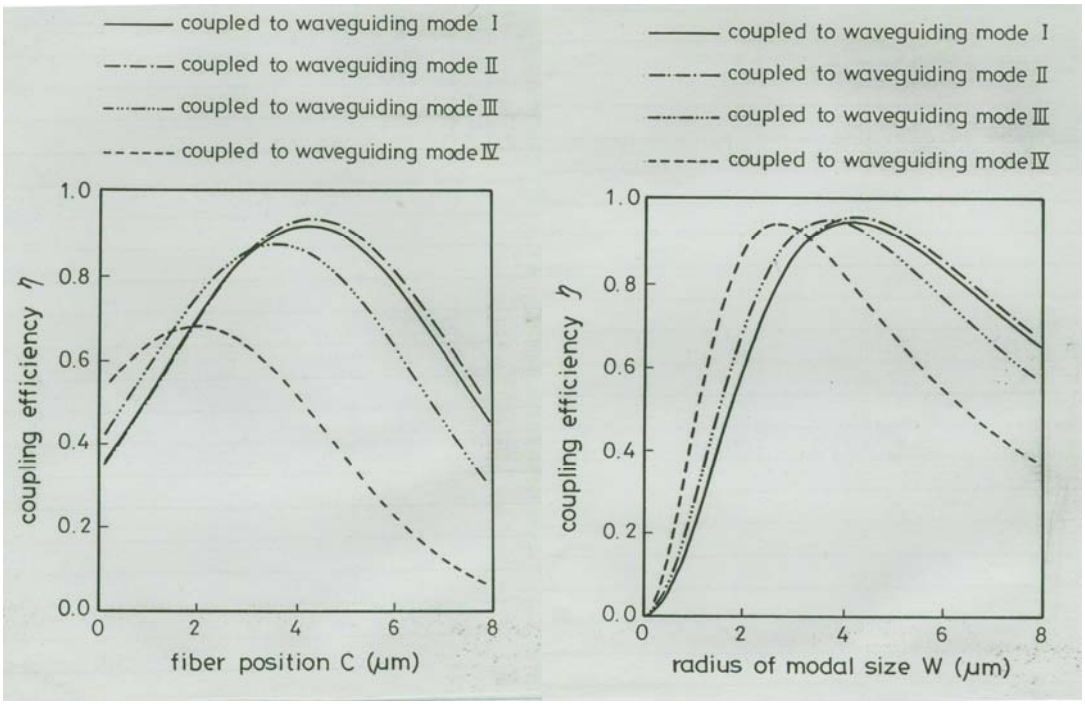

7-10 Theory of Crystals

Lattice: A periodical structure of atoms. Due to the periodicity of the lattice, we have $\varepsilon(\vec{r}+\vec{R})=\varepsilon(\vec{r})$. Furthermore, $\varepsilon(-\vec{r})=\varepsilon(\vec{r})$ and there exist several axes and planes of symmetry.

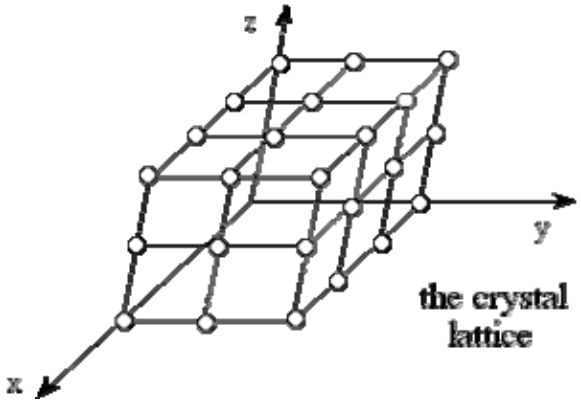

Primitive vectors: $\vec{a}_1=\vec{a},\ \vec{a}_2=\vec{b},\ \vec{a}_3=\vec{c}$

Translation vector: $\vec{R}=\alpha_1\vec{a}_1+\alpha_2\vec{a}_2+\alpha_3\vec{a}_3$, where $\alpha_1, \alpha_2, \alpha_3=0, \pm1, \pm2, \pm3,\ldots$.

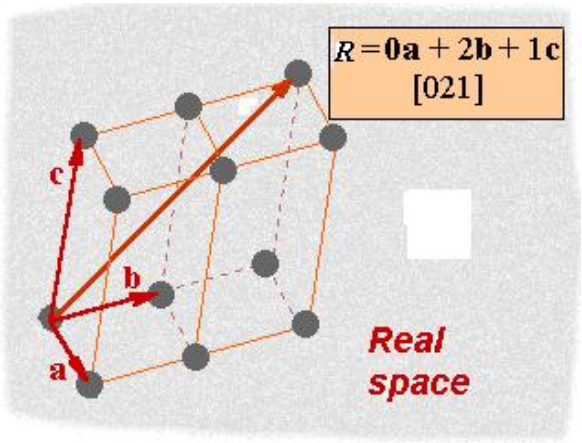

Primitive cell: The parallel hexagonal region composed of $\vec{a}_1,\ \vec{a}_2,\ and\ \vec{a}_3$.

Wigner-Seitz cell: The region bounded by bisecting line of two adjacent atoms.

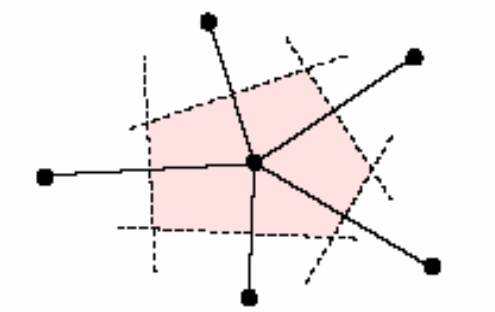

Reciprocal lattice: The Fourier domain of original lattice by optical diffraction or electron beam diffraction.

Reciprocal lattice primitive vectors: $\vec{b}_1 = \vec{a}^*,\ \vec{b}_2 = \vec{b}^*,\ and\ \vec{b}_3 = \vec{c}^*$.

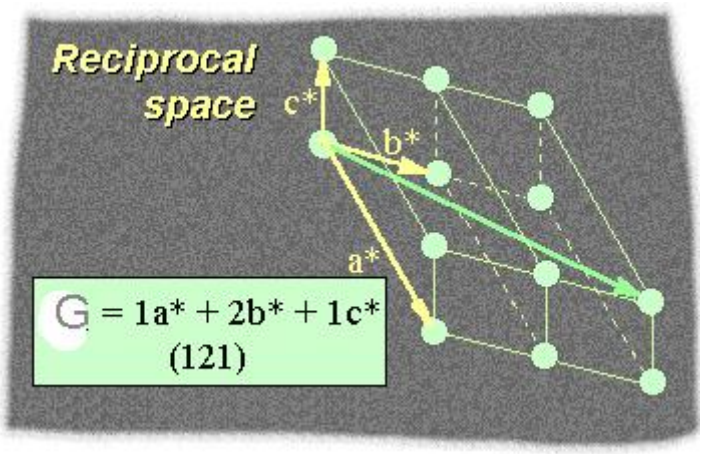

Translation vector in the reciprocal lattice: $\vec{G} = \beta_1\vec{b}_1 + \beta_2\vec{b}_2 + \beta_3\vec{b}_3$, where β_1, β_2, β_3=0, ±1, ±2, ±3,….

$\because \varepsilon(\vec{r}+\vec{R})=\varepsilon(\vec{r}),\quad \therefore \varepsilon(\vec{r}) = \sum_{\vec{G}} \bar{\varepsilon}(\vec{G})e^{i\vec{G}\cdot\vec{r}} = \varepsilon(\vec{r}+\vec{R}) = \sum_{\vec{G}} \bar{\varepsilon}(\vec{G})e^{i\vec{G}\cdot(\vec{r}+\vec{R})}$

$\Rightarrow$ **Bragg's diffraction law:** $\vec{G}\cdot\vec{R} = 2n\pi$. It implies $\vec{b}_j \cdot \vec{a}_i = 2\pi\delta_{ij}$.

Let $\vec{b}_1 = k(\vec{a}_2 \times \vec{a}_3)$, $\vec{b}_1 \cdot \vec{a}_1 = 2\pi \Rightarrow k = \dfrac{2\pi}{\vec{a}_1 \cdot (\vec{a}_2 \times \vec{a}_3)} \Rightarrow \vec{b}_1 = \dfrac{2\pi(\vec{a}_2 \times \vec{a}_3)}{\vec{a}_1 \cdot (\vec{a}_2 \times \vec{a}_3)}$

Similarly, $b_2 = 2\pi \dfrac{\vec{a}_3 \times \vec{a}_1}{\vec{a}_2 \cdot (\vec{a}_3 \times \vec{a}_1)}$ and $b_3 = 2\pi \dfrac{\vec{a}_1 \times \vec{a}_2}{\vec{a}_3 \cdot (\vec{a}_1 \times \vec{a}_2)}$

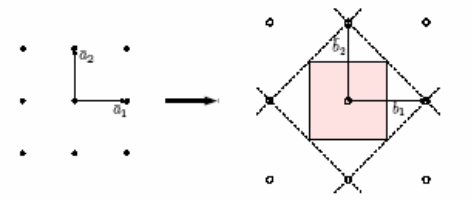

Square lattice and its reciprocal lattice

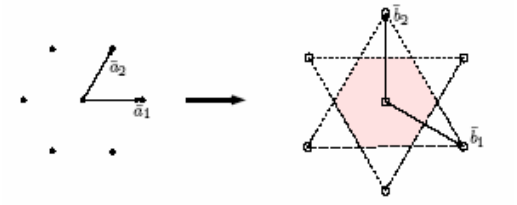

Hexagonal(triangular) lattice and its reciprocal lattice

Square lattice	$\bar{a}_1 = a\hat{x}$ $\bar{a}_2 = a\hat{y}$	$\bar{b}_1 = 2\pi/a\,\hat{x}$ $\bar{b}_2 = 2\pi/a\,\hat{y}$
Triangular lattice	$\bar{a}_1 = a\hat{x}$ $\bar{a}_2 = (\hat{x} + \sqrt{3}\hat{y})$	$\bar{b}_1 = 2\pi/a\,(\hat{x} - \sqrt{3}/3\,\hat{y})$ $\bar{b}_2 = 2\pi/a\,2\sqrt{3}/3\,\hat{y}$

Table Definition of $\bar{a}$ and $\bar{b}$ vectors for square and triangular (or hexagonal) lattice.

Brillouin Zones: Wigner-Seitz cells in the reciprocal lattice.

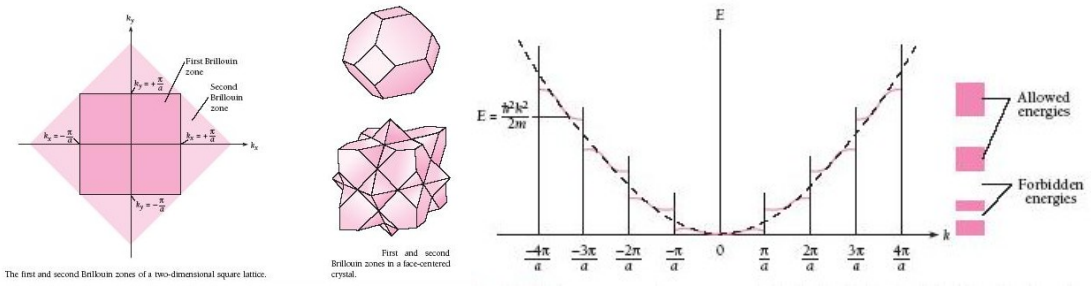

The first and second Brillouin zones of a two-dimensional square lattice.

First and second Brillouin zones in a face-centered crystal.

Band diagram: Describe the relation between the energy and the momentum.

In quantum mechanics, the energy of n photons is $E_{photon}=nhv=n\hbar\omega$ ($\propto\omega$ or v), the energy of n phonons is $E_{phonon}=(n+1/2)hv=(n+1/2)\hbar\omega$, where h is the Plank's constant, v is the frequency, $\hbar=h/2\pi$, and $\omega=2\pi v$. The downward transition of an electron between energy levels or bands may emit photons or phonons. The upward transition between energy levels or bands can absorb photons or phonons.

On the other hand, quantum mechanics shows that the momentum of an electron is $p=mv=h/\lambda=\hbar k\propto k$, where $k=2\pi/\lambda$ is the wavenumber of matter wave.

We can depict the relation of the energy ***E*** (or ***ω*)** of electrons in a crystal versus ***k*** (or ***p*)**. It is called *E-k* diagram or band diagram.

Eg. Two examples of band diagrams.

Direct bandgap: Eg. III-V compounds such as GaAs, Ga_xAl_{1-x} As.

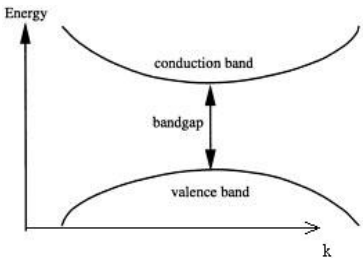

The downward transition of an electron in a crystal of the **direct bandgap** can emit photons. ($\because\triangle k=\triangle p=0$, $\therefore$ no variation in lattice momentum. All loss of energy due to downward transition must become radiation of photons).

Indirect bandgap: Eg. Crystalline Si.

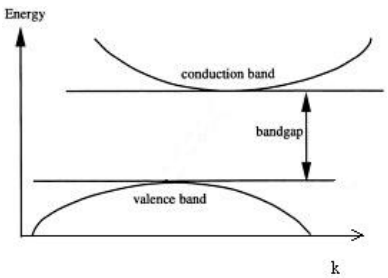

The downward transition of an electron in a crystal of the **indirect bandgap** can not emit photons, but it can cause lattice vibration and then generate heat or acoustic waves, etc. ($\because\triangle k\neq0\Leftrightarrow\triangle p\neq0$, There exists variation in lattice momentum. The loss of energy due to downward transition can become phonon radiation).

Note: Usually, crystalline Si can not emit photons. But porous Si and nano-structure cluster Si in SiO_2 can emit photons.

Lattice defects of crystals:

Vacancy:

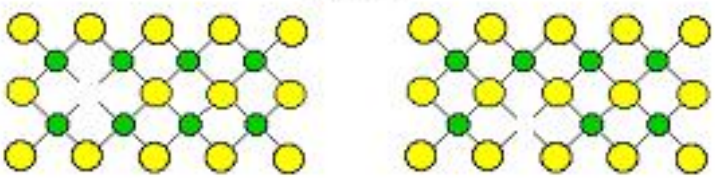

Interstitial impurity:

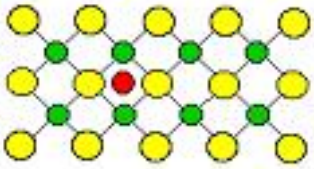

Substitution:

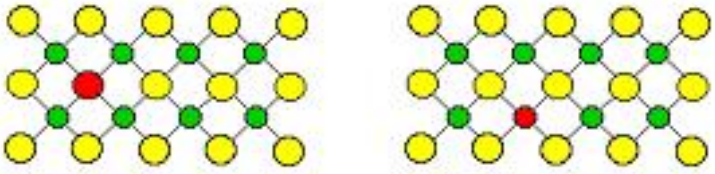

Antisite defect:

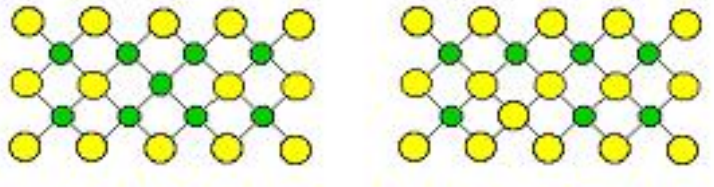

Dislocation:

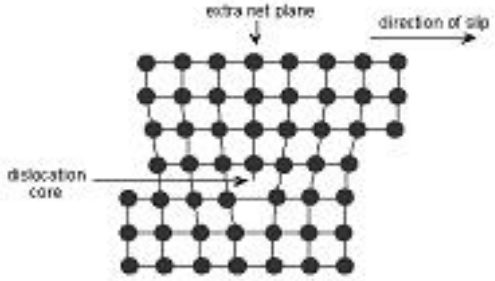

7-11 Theory of Photonic Crystals

Define the Fourier coefficients of periodical permittivity as follows.

$\varepsilon(\vec{r}) = \sum_G \bar{\varepsilon}(\vec{G}) e^{i\vec{G}\cdot\vec{r}}$, $\bar{\varepsilon}(\vec{G}) = \frac{1}{\Omega}\int_\Omega \varepsilon(\vec{r}) e^{-i\vec{G}\cdot\vec{r}} d\vec{r}$ $\frac{1}{\varepsilon(\vec{r})} = \sum_G \bar{\varepsilon}^{-1}(\vec{G}) e^{i\vec{G}\cdot\vec{r}}$, and $\bar{\varepsilon}^{-1}(\vec{G}) = \frac{1}{\Omega}\int_\Omega \frac{e^{-i\vec{k}\cdot\vec{r}}}{\varepsilon(\vec{r})} d\vec{r}$, where Ω denotes the surface of the elementary cell. Note that $\varepsilon(\vec{r}) = \varepsilon(-\vec{r})$ and $\bar{\varepsilon}(\vec{G}) = \bar{\varepsilon}(-\vec{G})$ for a crystal.

***H*-formulation:** $\nabla \times \left(\frac{1}{\varepsilon(\vec{r})} \nabla \times \vec{H}(\vec{r}) \right) = \frac{\omega^2}{c^2} \vec{H}(\vec{r})$, where $\vec{H}(\vec{r}) = \sum_{j=1}^{2} \hat{u}_j H_j(\vec{k}) e^{i\vec{k}\cdot\vec{r}}$ and $\hat{u}_j$ is the unit vector of the j^{th} coordinate basis ($\hat{u}_i \cdot \hat{u}_j = \delta_{ij}$ for the orthogonal coordinate system).

∵ Periodicities of the lattice and the reciprocal lattice, ∴ $\vec{H}(\vec{r}) = \vec{H}(\vec{r} + \vec{R})$ and

$$H_j(\vec{k}) e^{i\vec{k}\cdot\vec{r}} = H_j(\vec{k} + \vec{G}) e^{i(\vec{k}+\vec{G})\cdot\vec{r}} \Rightarrow \vec{H}(\vec{r}) = \sum_{\vec{G}} \sum_{j=1}^{2} \hat{u}_j H_{\vec{G},j}(\vec{k} + \vec{G}) e^{i(\vec{k}+\vec{G})\cdot\vec{r}} \equiv \sum_{\vec{G}} \sum_{j=1}^{2} \hat{u}_j H_{\vec{G},j} e^{i(\vec{k}+\vec{G})\cdot\vec{r}}$$

Substitute $\frac{1}{\varepsilon(\vec{r})} = \sum_G \bar{\varepsilon}^{-1}(\vec{G}) e^{i\vec{G}\cdot\vec{r}}$ and $\vec{H}(\vec{r}) = \sum_{\vec{G}} \sum_{j=1}^{2} \hat{u}_j H_{\vec{G},j} e^{i(\vec{k}+\vec{G})\cdot\vec{r}}$ into $\nabla \times \left(\frac{1}{\varepsilon(\vec{r})} \nabla \times \vec{H}(\vec{r}) \right) = \frac{\omega^2}{c^2} \vec{H}(\vec{r}) \Rightarrow$

$$-e^{i\vec{k}\cdot\vec{r}} \sum_{\vec{G},\vec{G}',j} \varepsilon^{-1}(\vec{G}') \; (\vec{k} + \vec{G} + \vec{G}') \times [(\vec{k} + \vec{G}) H_{\vec{G}',j} e^{i(\vec{G}+\vec{G}')\cdot\vec{r}} \times \hat{u}_j] = \frac{\omega^2}{c^2} e^{i\vec{k}\cdot\vec{r}} \sum_{\vec{G},j} H_{\vec{G},j} e^{i\vec{G}\cdot\vec{r}} \hat{u}_j$$

Multiply $e^{-i\vec{G}''\cdot\vec{r}}$ and divide $e^{i\vec{k}\cdot\vec{r}}$ at the both sides of the above equation, we have

$$-\sum_{\vec{G},\vec{G}',j} \varepsilon^{-1}(\vec{G}') \; (\vec{k} + \vec{G} + \vec{G}') \times [(\vec{k} + \vec{G}) H_{\vec{G}',j} e^{i(\vec{G}+\vec{G}'-\vec{G}'')\cdot\vec{r}} \times \hat{u}_j] = \frac{\omega^2}{c^2} \sum_{\vec{G},j} H_{\vec{G},j} e^{i(\vec{G}-\vec{G}'')\cdot\vec{r}} \hat{u}_j .$$

And integrate each term all over the whole cell. Utilizing

$$\int d\vec{r} \sum_{\vec{G},\vec{G}'} e^{i(\vec{G}+\vec{G}'-\vec{G}'')\cdot\vec{r}} = \begin{cases} \sum_{\vec{G}} (\cdots) \neq 0, & \vec{G} = \vec{G}'' - \vec{G}' \\ 0, & else \end{cases} \quad \text{and} \quad \int d\vec{r} \sum_{\vec{G}} e^{i(\vec{G}-\vec{G}'')\cdot\vec{r}} = \begin{cases} \neq 0, & \vec{G} = \vec{G}'' \\ 0, & else \end{cases}$$

we have $-\sum_{\vec{G}',j} \varepsilon^{-1}(\vec{G}'' - \vec{G}) \; (\vec{k} + \vec{G}'') \times [(\vec{k} + \vec{G}) H_{\vec{G}',j} \times \hat{u}_j] = \frac{\omega^2}{c^2} \sum_j H_{\vec{G}',j} \hat{u}_j$

And then replace $\vec{G}''$ by $\vec{G}'$ at the left side and replace $\vec{G}'$ by $\vec{G}$ in the right side.

It is obtained: $-\sum_{\vec{G}',j}\varepsilon^{-1}(\vec{G}'-\vec{G})\ (\vec{k}+\vec{G}')\times[(\vec{k}+\vec{G})H_{\vec{G}',j}\times\hat{u}_j]=\frac{\omega^2}{c^2}\sum_j H_{\vec{G},j}\hat{u}_j$.

We take the inner products of the above equation with $\hat{u}_1$ and $\hat{u}_2$, respectively. By

$\vec{A}\times(\vec{B}\times\vec{C})=(\vec{A}\cdot\vec{C})\vec{B}-(\vec{A}\cdot\vec{B})\vec{C}$, $[\vec{A}\times(\vec{B}\times\vec{C})]\cdot\vec{D}=(\vec{A}\cdot\vec{C})\vec{B}\cdot\vec{D}-(\vec{A}\cdot\vec{B})\vec{C}\cdot\vec{D}\Rightarrow$

Eigenvalue problems: Given a plane wave $e^{i(\vec{k}+\vec{G})\cdot\vec{r}}$, we can obtain the eigenvalue ω and depict the band diagram.

$$\sum_{\vec{G}'}\varepsilon^{-1}(\vec{G}-\vec{G}')(\vec{k}+\vec{G})\cdot(\vec{k}+\vec{G}')H_{\vec{G}',1}=\frac{\omega^2}{c^2}H_{\vec{G},1}\quad (TE\ wave)$$

$$\sum_{\vec{G}'}\varepsilon^{-1}(\vec{G}-\vec{G}')\left|\vec{k}+\vec{G}\right|\cdot\left|\vec{k}+\vec{G}'\right|H_{\vec{G}',2}=\frac{\omega^2}{c^2}H_{\vec{G},2}\quad (TM\ wave)$$

Eg. Photonic crystals with (a) a square lattice, (b) a triangular lattice. Other parameters are ε_a=1, ε_b=12, R_c/a=0.35.

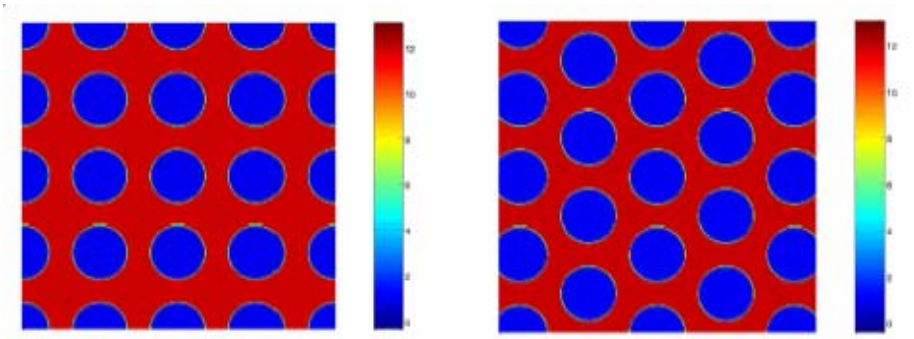

(a) Square lattice ($f_r = 38.48\%$). (b) Triangular lattice ($f_r = 44.43\%$).

Reciprocal lattices:

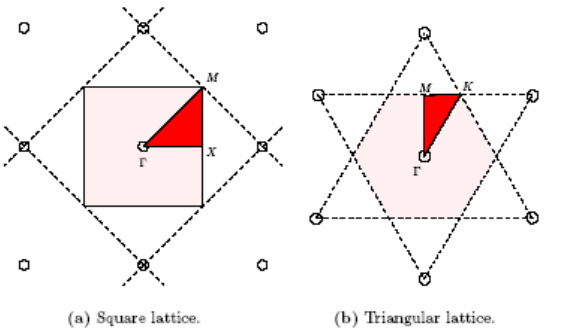

(a) Square lattice. (b) Triangular lattice.

Square lattice: $\Gamma\to(k_x=k_y=0)$, $X\to(k_x=\frac{\pi}{a},\ k_y=0)$, $M\to(k_x=k_y=\frac{\pi}{a})$

Hexagonal lattice: $\Gamma\to(k_x=k_y=0)$, $K\to(k_x=k_y=\frac{2\pi}{3a})$, $M\to(k_x=\frac{2\pi}{3a},k_y=0)$

For a 2D photonic crystal made of circular cylinders,

$$\bar{\varepsilon}(\vec{G}) = \begin{cases} \varepsilon_a f_r + \varepsilon_b (1 - f_r), & \vec{G} = 0 \\ (\varepsilon_a - \varepsilon_b) f_r \dfrac{2J_1(|\vec{G}|R_c)}{|\vec{G}|R_c}, & eleswhere \end{cases}, \text{ where } f_r = \begin{cases} \dfrac{\pi R_c}{a^2}, & square\ lattice \\ \dfrac{2\pi R_c}{\sqrt{3}a^2}, & hexagonal\ lattice \end{cases}.$$

Eg. The band structures of the 2D square-lattice photonic crystal with the lattice constant is *a*=0.5*μm*. The radius of the pillar is R_c=225*nm*. And the refractive index of the pillar is 3.16227766.

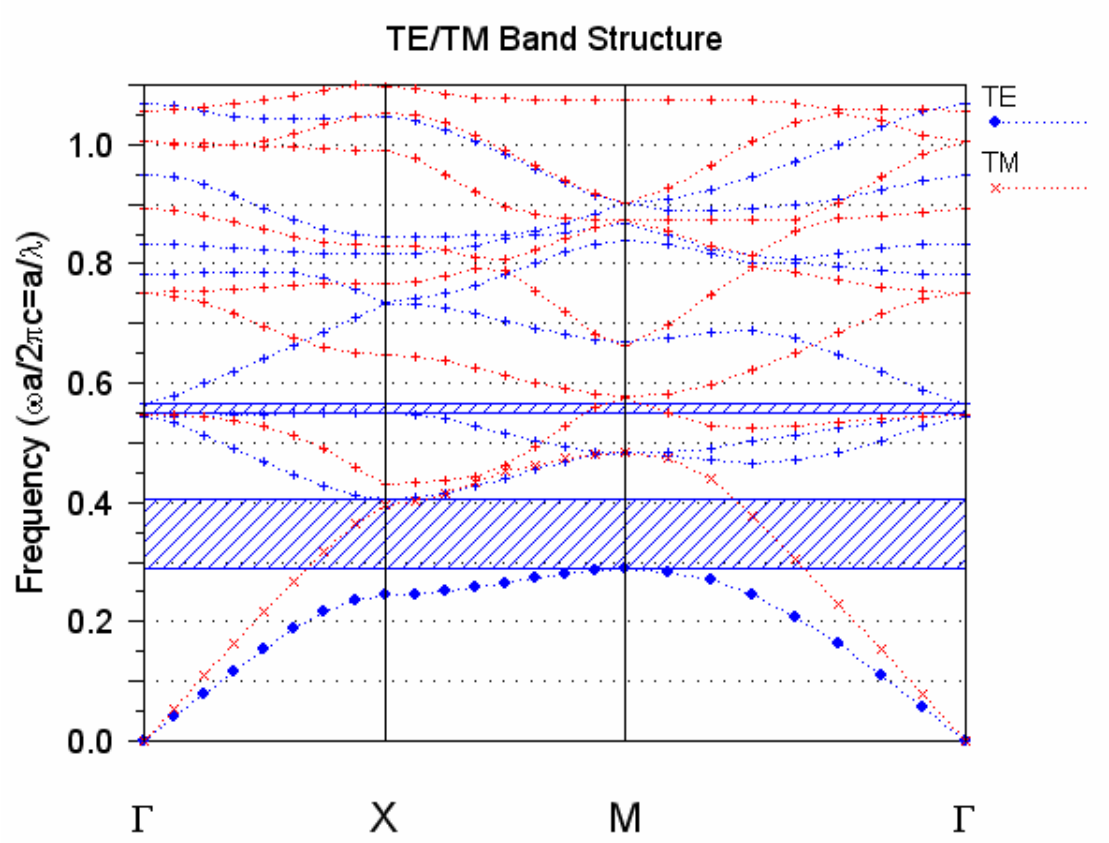

Eg. An example of 3D photonic crystal.

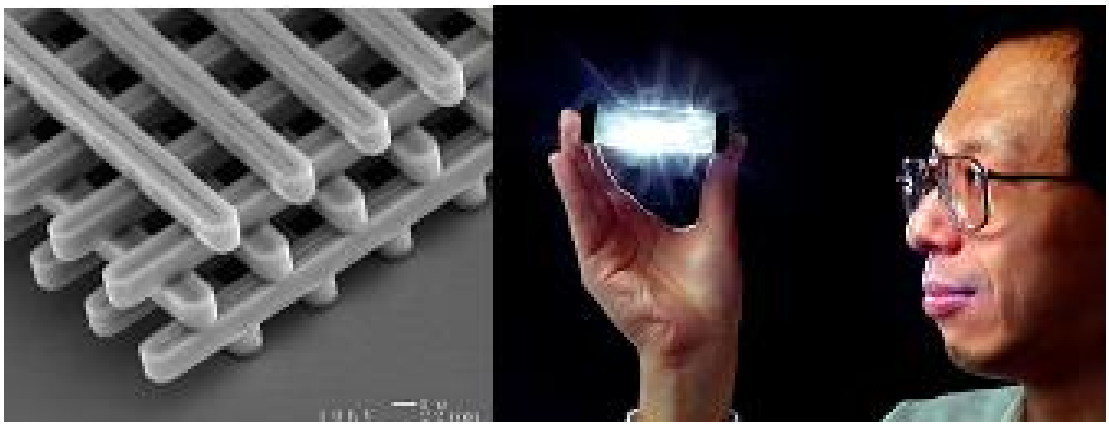

Comparison between the conventional optical waveguide devices and the photonic crystal waveguide devices:

1. The conventional optical waveguides made of dielectrics are weakly guided. There exist large power losses in the wide-angle bends/branches. However, the same structures made of line-defect photonic crystals give little losses because the lights were trapped by the defects of the photonic crystals.
2. Most of the conventional optical waveguide devices can be easily modulated by **E-O effect**, **A-O effect**, and so on. But only a few photonic crystal waveguide devices can be modulated.

Eg. A laser beam passes a *T*-junction of a photonic crystal. (by C. -C. Tsai蔡佳辰, T. –C. Weng翁宗誠, Y. –L. Kuo郭奕麟, C. –W. Kao高智偉, K. –Y. Chen陳奎元, *et al*.)

a =1μm, $2r_c$=0.45μm, n_c=3.16227766, a/λ=0.4081632 (λ=2.45μm)

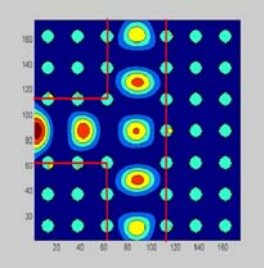

Eg. Simulation of light propagating along 90°-bent photonic crystal waveguides. (by C. -C. Tsai, T. –C. Weng, K. –Y. Kuo, C. –W. Kao, K. –Y. Chen, *et al*.)

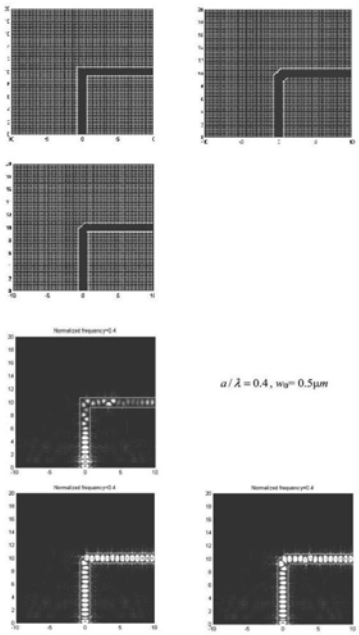

The photonic crystal devices can be simulated by FDTD method.

7-12 FDTD Method

3D Full-vector FDTD method (by Kane S. Yee)

Maxwell's equations in the source-free region: $\nabla \times \vec{H} = \sigma \vec{E} + \varepsilon \frac{\partial \vec{E}}{\partial t}$, $\nabla \times \vec{E} = \mu \frac{\partial \vec{H}}{\partial t}$

$$\Rightarrow \sigma E_x + \varepsilon \frac{\partial E_x}{\partial t} = \frac{\partial H_z}{\partial y} - \frac{\partial H_y}{\partial z}, \quad \sigma E_y + \varepsilon \frac{\partial E_y}{\partial t} = \frac{\partial H_x}{\partial z} - \frac{\partial H_z}{\partial x},$$

$$\sigma E_z + \varepsilon \frac{\partial E_z}{\partial t} = \frac{\partial H_y}{\partial x} - \frac{\partial H_x}{\partial y},$$

$$\mu \frac{\partial H_x}{\partial t} = \frac{\partial E_y}{\partial z} - \frac{\partial E_z}{\partial y}, \quad \mu \frac{\partial H_y}{\partial t} = \frac{\partial E_z}{\partial x} - \frac{\partial E_x}{\partial z}, \quad \mu \frac{\partial H_z}{\partial t} = \frac{\partial E_x}{\partial y} - \frac{\partial E_y}{\partial x}$$

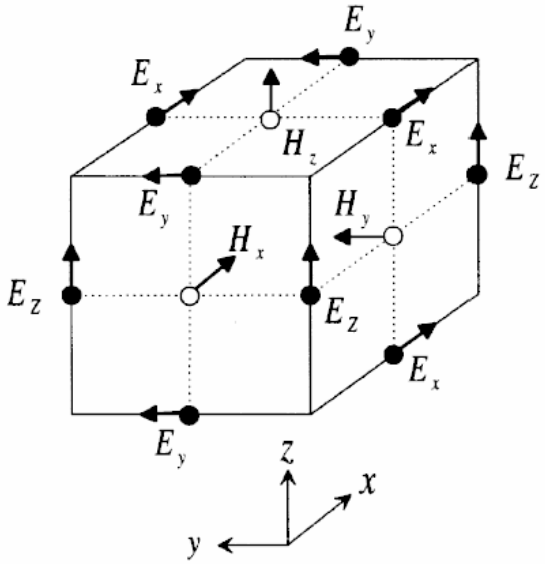

(Yee's FDTD cell, 1966)

According to Yee's algorithm, define the following notations: $E(i\triangle x, j\triangle y, k\triangle z, l\triangle t) \equiv E(i,j,k,l) \equiv E^l(i,j,k)$ and $H(i\triangle x, j\triangle y, k\triangle z, l\triangle t) \equiv H(i,j,k,l) \equiv H^l(i,j,k)$. We have

$$\frac{\partial E_x}{\partial t} \approx \frac{E_x(i+\frac{1}{2}, j, k, l+1) - E_x(i+\frac{1}{2}, j, k, l)}{\Delta t},$$

$$\frac{\partial E_y}{\partial t} \approx \frac{E_y(i, j+\frac{1}{2}, k, l+1) - E_y(i, j+\frac{1}{2}, k, l)}{\Delta t},$$

$$\frac{\partial E_z}{\partial t} \approx \frac{E_z(i, j, k+\frac{1}{2}, l+1) - E_z(i, j, k+\frac{1}{2}, l)}{\Delta t},$$

$$\frac{\partial E_x}{\partial y} \approx \frac{E_x(i+\frac{1}{2},j,k,l) - E_x(i+\frac{1}{2},j-1,k,l)}{\Delta y},$$

$$\frac{\partial E_x}{\partial z} \approx \frac{E_x(i+\frac{1}{2},j,k,l) - E_x(i+\frac{1}{2},j,k-1,l)}{\Delta z},$$

$$\frac{\partial E_y}{\partial x} \approx \frac{E_y(i,j+\frac{1}{2},k,l) - E_y(i-1,j+\frac{1}{2},k,l)}{\Delta x},$$

$$\frac{\partial E_y}{\partial z} \approx \frac{E_y(i,j+\frac{1}{2},k,l) - E_y(i,j+\frac{1}{2},k-1,l)}{\Delta z},$$

$$\frac{\partial E_z}{\partial x} \approx \frac{E_z(i,j,k+\frac{1}{2},l) - E_z(i-1,j,k+\frac{1}{2},l)}{\Delta x},$$

$$\frac{\partial E_z}{\partial y} \approx \frac{E_z(i,j,k+\frac{1}{2},l) - E_z(i,j-1,k+\frac{1}{2},l)}{\Delta y},$$

But

$$\frac{\partial H_x}{\partial t} \approx \frac{H_x(i,j+\frac{1}{2},k+\frac{1}{2},l+\frac{1}{2}) - H_x(i,j+\frac{1}{2},k+\frac{1}{2},l-\frac{1}{2})}{\Delta t},$$

$$\frac{\partial H_y}{\partial t} \approx \frac{H_y(i+\frac{1}{2},j,k+\frac{1}{2},l+\frac{1}{2}) - H_y(i+\frac{1}{2},j,k+\frac{1}{2},l-\frac{1}{2})}{\Delta t},$$

$$\frac{\partial H_z}{\partial t} \approx \frac{H_z(i+\frac{1}{2},j+\frac{1}{2},k,l+\frac{1}{2}) - H_z(i+\frac{1}{2},j+\frac{1}{2},k,l-\frac{1}{2})}{\Delta t},$$

$$\frac{\partial H_x}{\partial y} \approx \frac{H_x(i,j+\frac{1}{2},k+\frac{1}{2},l-\frac{1}{2}) - H_x(i,j-\frac{1}{2},k+\frac{1}{2},l-\frac{1}{2})}{\Delta y},$$

$$\frac{\partial H_x}{\partial z} \approx \frac{H_x(i,j+\frac{1}{2},k+\frac{1}{2},l-\frac{1}{2}) - H_x(i,j+\frac{1}{2},k-\frac{1}{2},l-\frac{1}{2})}{\Delta z},$$

$$\frac{\partial H_y}{\partial x} \approx \frac{H_y(i+\frac{1}{2},j,k+\frac{1}{2},l-\frac{1}{2}) - H_y(i-\frac{1}{2},j,k+\frac{1}{2},l-\frac{1}{2})}{\Delta x},$$

$$\frac{\partial H_y}{\partial z} \approx \frac{H_y(i+\frac{1}{2},j,k+\frac{1}{2},l-\frac{1}{2}) - H_y(i+\frac{1}{2},j,k-\frac{1}{2},l-\frac{1}{2})}{\Delta z},$$

$$\frac{\partial H_z}{\partial x} \approx \frac{H_z(i+\frac{1}{2},j+\frac{1}{2},k,l-\frac{1}{2}) - H_z(i-\frac{1}{2},j+\frac{1}{2},k,l-\frac{1}{2})}{\Delta x},$$

$$\frac{\partial H_z}{\partial y} \approx \frac{H_z(i+\frac{1}{2},j+\frac{1}{2},k,l-\frac{1}{2}) - H_z(i+\frac{1}{2},j-\frac{1}{2},k,l-\frac{1}{2})}{\Delta y}$$

$$\Rightarrow$$

$$E_x^{l+1}(i+\frac{1}{2},j,k) = C_a(i+\frac{1}{2},j,k)E_x^l(i+\frac{1}{2},j,k) + C_b(i+\frac{1}{2},j,k)\cdot$$
$$\left[\frac{H_z^{l-\frac{1}{2}}(i+\frac{1}{2},j+\frac{1}{2},k) - H_z^{l-\frac{1}{2}}(i+\frac{1}{2},j-\frac{1}{2},k)}{\Delta y} - \frac{H_y^{l-\frac{1}{2}}(i+\frac{1}{2},j,k+\frac{1}{2}) - H_y^{l-\frac{1}{2}}(i+\frac{1}{2},j,k-\frac{1}{2})}{\Delta z}\right],$$

$$E_y^{l+1}(i,j+\frac{1}{2},k) = C_a(i,j+\frac{1}{2},k)E_y^l(i,j+\frac{1}{2},k) + C_b(i,j+\frac{1}{2},k)\cdot$$
$$\left[\frac{H_x^{l-\frac{1}{2}}(i,j+\frac{1}{2},k+\frac{1}{2}) - H_x^{l-\frac{1}{2}}(i,j+\frac{1}{2},k-\frac{1}{2})}{\Delta z} - \frac{H_z^{l-\frac{1}{2}}(i+\frac{1}{2},j+\frac{1}{2},k) - H_z^{l-\frac{1}{2}}(i-\frac{1}{2},j+\frac{1}{2},k)}{\Delta x}\right],$$

$$E_z^{l+1}(i,j,k+\frac{1}{2}) = C_a(i,j,k+\frac{1}{2})E_z^l(i,j,k+\frac{1}{2}) + C_b(i,j,k+\frac{1}{2})\cdot$$
$$\left[\frac{H_y^{l-\frac{1}{2}}(i+\frac{1}{2},j,k+\frac{1}{2}) - H_y^{l-\frac{1}{2}}(i-\frac{1}{2},j,k+\frac{1}{2})}{\Delta x} - \frac{H_x^{l-\frac{1}{2}}(i,j+\frac{1}{2},k+\frac{1}{2}) - H_x^{l-\frac{1}{2}}(i,j-\frac{1}{2},k+\frac{1}{2})}{\Delta y}\right],$$

$$H_x^{l+\frac{1}{2}}(i,j+\frac{1}{2},k+\frac{1}{2}) = H_x^{l-\frac{1}{2}}(i,j+\frac{1}{2},k+\frac{1}{2}) + D_b(i,j+\frac{1}{2},k+\frac{1}{2})\cdot$$
$$\left[-\frac{E_z^l(i,j+1,k+\frac{1}{2}) - E_z^l(i,j,k+\frac{1}{2})}{\Delta y} + \frac{E_y^l(i,j+\frac{1}{2},k+1) - E_y^l(i,j+\frac{1}{2},k)}{\Delta z}\right],$$

$$H_y^{l+\frac{1}{2}}(i+\frac{1}{2},j,k+\frac{1}{2}) = H_y^{l-\frac{1}{2}}(i+\frac{1}{2},j,k+\frac{1}{2}) + D_b(i+\frac{1}{2},j,k+\frac{1}{2})\cdot$$
$$\left[\frac{E_z^l(i+1,j,k+\frac{1}{2}) - E_z^l(i,j,k+\frac{1}{2})}{\Delta x} - \frac{E_x^l(i+\frac{1}{2},j,k+1) - E_x^l(i+\frac{1}{2},j,k)}{\Delta z}\right],$$

$$H_z^{l+\frac{1}{2}}(i+\frac{1}{2},j+\frac{1}{2},k) = H_z^{l-\frac{1}{2}}(i+\frac{1}{2},j+\frac{1}{2},k) + D_b(i+\frac{1}{2},j+\frac{1}{2},k)\cdot$$
$$\left[\frac{E_x^l(i+\frac{1}{2},j+1,k) - E_x^l(i+\frac{1}{2},j,k)}{\Delta y} - \frac{E_y^l(i+1,j+\frac{1}{2},k) - E_y^l(i,j+\frac{1}{2},k)}{\Delta x}\right],$$

where $C_a(i,j,k) = \dfrac{2\varepsilon(i,j,k) - \sigma(i,j,k)\Delta t}{2\varepsilon(i,j,k) + \sigma(i,j,k)\Delta t}$, $C_b(i,j,k) = \dfrac{2\Delta t}{2\varepsilon(i,j,k) + \sigma(i,j,k)\Delta t}$,

and $D_b(i,j,k) = \dfrac{\Delta t}{\mu(i,j,k)}$

$$\text{Power distribution} \propto \left|\vec{E}\right|^2 = (E_x{}^2 + E_y{}^2 + E_z{}^2)$$

3D Scalar FDTD method (by Dr. Wei-Ping Huang)

Wave equation: $\nabla^2\Psi - \dfrac{n^2}{c^2}\dfrac{\partial^2\Psi}{\partial t^2} = \dfrac{\partial^2\Psi}{\partial x^2} + \dfrac{\partial^2\Psi}{\partial y^2} + \dfrac{\partial^2\Psi}{\partial z^2} - \dfrac{n^2}{c^2}\dfrac{\partial^2\Psi}{\partial t^2} = 0$

Notation: $\Psi(i\Delta x, j\Delta y, k\Delta z, l\Delta t) = \Psi^l(i,j,k)$, $\dfrac{\partial^2\Psi}{\partial x^2} = \dfrac{\Psi^l(i+1,j,k) - 2\Psi^l(i,j,k) + \Psi^l(i-1,j,k)}{\Delta x^2}$

$$\Rightarrow \Psi^{l+1}(i,j,k) = 2\cdot[1 - \frac{\delta_x{}^2 + \delta_y{}^2 + \delta_z{}^2}{n^2(i,j,k)}]\cdot\Psi^l(i,j,k) - \Psi^{l-1}(i,j,k)$$

$$+\frac{\delta_x{}^2}{n^2(i,j,k)}\cdot[\Psi^l(i+1,j,k) + \Psi^l(i-1,j,k)] + \frac{\delta_y{}^2}{n^2(i,j,k)}\cdot[\Psi^l(i,j+1,k) + \Psi^l(i,j-1,k)]$$

$$+\frac{\delta_z{}^2}{n^2(i,j,k)}\cdot[\Psi^l(i,j,k+1) + \Psi^l(i,j,k-1)]$$

where $\delta_x = \dfrac{c\Delta t}{\Delta x}$, $\delta_y = \dfrac{c\Delta t}{\Delta y}$, $\delta_z = \dfrac{c\Delta t}{\Delta z}$, $\Delta t \le \dfrac{1}{v_{\max}\sqrt{\dfrac{1}{\Delta x^2} + \dfrac{1}{\Delta y^2} + \dfrac{1}{\Delta z^2}}}$

For the ***z*-propagational initial sinusoidal field:** $\Psi^l(i,j,0) = \Phi(i,j,0)\sin(\dfrac{2cl\pi\Delta t}{\lambda})$

Mur's First-Order Absorbing Boundary Conditions:

$x=0,\quad \Psi^{l+1}(0,j,k)=\Psi^{l}(1,j,k)+\dfrac{c\Delta t-\Delta x}{c\Delta t+\Delta x}\cdot[\Psi^{l+1}(1,j,k)-\Psi^{l}(0,j,k)]$

$x=I\triangle x,\quad \Psi^{l+1}(I,j,k)=\Psi^{l}(I-1,j,k)+\dfrac{c\Delta t-\Delta x}{c\Delta t+\Delta x}\cdot[\Psi^{l+1}(I-1,j,k)-\Psi^{l}(I,j,k)]$

$y=0,\quad \Psi^{l+1}(i,0,k)=\Psi^{l}(i,1,k)+\dfrac{c\Delta t-\Delta y}{c\Delta t+\Delta y}\cdot[\Psi^{l+1}(i,1,k)-\Psi^{l}(i,0,k)]$

$y=J\triangle y,\quad \Psi^{l+1}(i,J,k)=\Psi^{l}(i,J-1,k)+\dfrac{c\Delta t-\Delta y}{c\Delta t+\Delta y}\cdot[\Psi^{l+1}(i,J-1,k)-\Psi^{l}(i,J,k)]$

$z=0,\quad \Psi^{l+1}(i,j,0)=\Psi^{l}(i,j,0)+\dfrac{c\Delta t-\Delta z}{c\Delta t+\Delta z}\cdot[\Psi^{l+1}(i,j,1)-\Psi^{l}(i,j,0)]$

$z=K\triangle z,\quad \Psi^{l+1}(i,j,K)=\Psi^{l}(i,j,K-1)+\dfrac{c\Delta t-\Delta z}{c\Delta t+\Delta z}\cdot[\Psi^{l+1}(i,j,K-1)-\Psi^{l}(i,j,K)]$

3D Semi-vector FDTD method (by Dr. Wei-Ping Huang)

$$E_x^{\,l+1}(i,j,k)=2\cdot\{1-\frac{[2-\frac{T(i+1,j,k)+T(i-1,j,k)}{2}]\cdot\delta_x^{\,2}+\delta_y^{\,2}+\delta_z^{\,2}}{n^2(i,j,k)}\}\cdot E_x^{\,l}(i,j,k)-E_x^{\,l-1}(i,j,k)$$

$$+\frac{\delta_x^{\,2}}{n^2(i,j,k)}\cdot[T(i+1,j,k)\cdot E_x^{\,l}(i+1,j,k)+T(i-1,j,k)\cdot E_x^{\,l}(i-1,j,k)]$$

$$+\frac{\delta_y^{\,2}}{n^2(i,j,k)}\cdot[E_x^{\,l}(i,j+1,k)+E_x^{\,l}(i,j-1,k)]+\frac{\delta_z^{\,2}}{n^2(i,j,k)}\cdot[E_x^{\,l}(i,j,k+1)+E_x^{\,l}(i,j,k-1)]$$

$$E_y^{\,l+1}(i,j,k)=2\cdot\{1-\frac{\delta_x^{\,2}+[2-\frac{T(i,j+1,k)+T(i,j-1,k)}{2}]\cdot\delta_y^{\,2}+\delta_z^{\,2}}{n^2(i,j,k)}\}\cdot E_y^{\,l}(i,j,k)-E_y^{\,l-1}(i,j,k)$$

$$+\frac{\delta_x^{\,2}}{n^2(i,j,k)}\cdot[E_y^{\,l}(i+1,j,k)+E_y^{\,l}(i-1,j,k)]+\frac{\delta_z^{\,2}}{n^2(i,j,k)}\cdot[E_y^{\,l}(i,j,k+1)+E_y^{\,l}(i,j,k-1)]$$

$$+\frac{\delta_y^{\,2}}{n^2(i,j,k)}\cdot[T(i,j+1,k)\cdot E_y^{\,l}(i,j+1,k)+T(i,j-1,k)\cdot E_y^{\,l}(i,j-1,k)]$$

where $T(i\pm1,j,k)=\dfrac{2n^2(i\pm1,j,k)}{n^2(i\pm1,j,k)+n^2(i,j,k)}$ and $T(i,j\pm1,k)=\dfrac{2n^2(i,j\pm1,k)}{n^2(i,j\pm1,k)+n^2(i,j,k)}$

Perfectly matched layer (PML) boundary condition for the scalar and the semi-vector FDTD methods: (by Dr. Wei-Ping Huang)

In the *x*-direction:

$$\Psi^{l+1}(i,j,k) = -\Psi^{l-1}(i,j,k) + 2\left[1 - \frac{\delta_y^{\,2} + \delta_z^{\,2}}{n^2(i,j,k)}\right]\Psi^{l}(i,j,k)$$

$$+ \frac{\delta_x^{\,2}}{n^2(i,j,k)}\left[D_{2x}{}^{l+\frac{1}{2}}(i,j,k) - D_{2x}{}^{l-\frac{1}{2}}(i,j,k)\right] + \frac{\delta_y^{\,2}}{n^2(i,j,k)}\left[\Psi^{l}(i,j+1,k) + \Psi^{l}(i,j-1,k)\right]$$

$$+ \frac{\delta_z^{\,2}}{n^2(i,j,k)}\left[\Psi^{l}(i,j,k+1) + \Psi^{l}(i,j,k-1)\right],$$

where $\delta_x = \dfrac{c\Delta t}{\Delta x}$, $\delta_y = \dfrac{c\Delta t}{\Delta y}$, $\delta_z = \dfrac{c\Delta t}{\Delta z}$

$$D_{1x}{}^{l+1}(i+1,j,k) = \frac{a_x - \dfrac{\sigma_x \cdot \Delta t}{\varepsilon_0 n^2(i+1,j,k)}}{a_x + \dfrac{\sigma_x \cdot \Delta t}{\varepsilon_0 n^2(i+1,j,k)}} \cdot D_{1x}{}^{l-1}(i+1,j,k)$$

$$+ \frac{1}{a_x + \dfrac{\sigma_x \cdot \Delta t}{\varepsilon_0 n^2(i+1,j,k)}} \cdot \left[\Psi^{l}(i+1,j,k) - \Psi^{l}(i,j,k)\right]$$

$$D_{2x}{}^{l+1}(i,j,k) = \frac{a_x - \dfrac{\sigma_x \cdot \Delta t}{\varepsilon_0 n^2(i+1,j,k)}}{a_x + \dfrac{\sigma_x \cdot \Delta t}{\varepsilon_0 n^2(i+1,j,k)}} \cdot D_{2x}{}^{l-1}(i,j,k)$$

$$+ \frac{1}{a_x + \dfrac{\sigma_x \cdot \Delta t}{\varepsilon_0 n^2(i+1,j,k)}} \cdot \left[D_{1x}{}^{l+1}(i+1,j,k) - D_{1x}{}^{l+1}(i-1,j,k)\right.$$

$$\left. - D_{1x}{}^{l-1}(i+1,j,k) + D_{1x}{}^{l-1}(i-1,j,k)\right]$$

$$\sigma_x(x) = \left(\frac{x}{d}\right)^m \sigma_{x\max} = -\left(\frac{x}{d}\right)^m \frac{n_x^{\,2}\varepsilon_0 c(m+1)\ln(R_0)}{2d}$$

$d = n_x \Delta x$: Thickness of *PML*, *m*: order

R_0: Reflection from *PML* at normal incidence

n_x=8, R_0=10^{-2}, *m*=4

In the *y*-direction:

$$\Psi^{l+1}(i,j,k) = -\Psi^{l-1}(i,j,k) + 2\left[1 - \frac{\delta_x^{\,2} + \delta_z^{\,2}}{n^2(i,j,k)}\right]\Psi^{l}(i,j,k)$$

$$+ \frac{\delta_x^{\,2}}{n^2(i,j,k)}\left[\Psi^{l}(i+1,j,k) + \Psi^{l}(i-1,j,k)\right] + \frac{\delta_y^{\,2}}{n^2(i,j,k)}\left[D_{2y}{}^{l+\frac{1}{2}}(i,j,k) - D_{2y}{}^{l-\frac{1}{2}}(i,j,k)\right]$$

$$+ \frac{\delta_z^{\,2}}{n^2(i,j,k)}\left[\Psi^{l}(i,j,k+1) + \Psi^{l}(i,j,k-1)\right]$$

where $\delta_x = \dfrac{c\Delta t}{\Delta x}$, $\delta_y = \dfrac{c\Delta t}{\Delta y}$, $\delta_z = \dfrac{c\Delta t}{\Delta z}$

$$D_{1y}{}^{l+1}(i,j+1,k) = \frac{a_y - \dfrac{\sigma_y \cdot \Delta t}{\varepsilon_0 n^2(i,j+1,k)}}{a_y + \dfrac{\sigma_y \cdot \Delta t}{\varepsilon_0 n^2(i,j+1,k)}} \cdot D_{1y}{}^{l-1}(i,j+1,k)$$

$$+ \frac{1}{a_y + \dfrac{\sigma_y \cdot \Delta t}{\varepsilon_0 n^2(i,j+1,k)}} \cdot \left[\Psi^{l}(i,j+1,k) - \Psi^{l}(i,j,k)\right]$$

$$D_{2y}{}^{l+1}(i,j,k) = \frac{a_y - \dfrac{\sigma_y \cdot \Delta t}{\varepsilon_0 n^2(i,j+1,k)}}{a_y + \dfrac{\sigma_y \cdot \Delta t}{\varepsilon_0 n^2(i,j+1,k)}} \cdot D_{2y}{}^{l-1}(i,j,k)$$

$$+ \frac{1}{a_y + \dfrac{\sigma_y \cdot \Delta t}{\varepsilon_0 n^2(i,j+1,k)}} \cdot \left[D_{1y}{}^{l+1}(i,j+1,k) - D_{1y}{}^{l+1}(i,j-1,k)\right.$$

$$\left. - D_{1y}{}^{l-1}(i,j+1,k) + D_{1y}{}^{l-1}(i,j-1,k)\right]$$

$$\sigma_y(y) = \left(\frac{y}{d}\right)^m \sigma_{y\max} = -\left(\frac{y}{d}\right)^m \frac{n_y{}^2 \varepsilon_0 c(m+1)\ln(R_0)}{2d}$$

$d = n_y \Delta y$: Thickness of *PML*, *m*: order

R_0: Reflection from *PML* at normal incidence

n_y=8, R_0=10^{-2}, *m*=4

In the z-direction:

$$\Psi^{l+1}(i,j,k) = -\Psi^{l-1}(i,j,k) + 2\left[1 - \frac{\delta_x^{\,2} + \delta_y^{\,2}}{n^2(i,j,k)}\right]\Psi^{l}(i,j,k)$$

$$+ \frac{\delta_x^{\,2}}{n^2(i,j,k)}\left[\Psi^{l}(i+1,j,k) + \Psi^{l}(i-1,j,k)\right] + \frac{\delta_y^{\,2}}{n^2(i,j,k)}\left[\Psi^{l}(i,j+1,k) + \Psi^{l}(i,j-1,k)\right]$$

$$+ \frac{\delta_z^{\,2}}{n^2(i,j,k)}\left[D_{2z}{}^{l+\frac{1}{2}}(i,j,k) - D_{2z}{}^{l-\frac{1}{2}}(i,j,k)\right]$$

where $\delta_x = \dfrac{c\Delta t}{\Delta x}$, $\delta_y = \dfrac{c\Delta t}{\Delta y}$, $\delta_z = \dfrac{c\Delta t}{\Delta z}$

$$D_{1z}{}^{l+1}(i,j,k+1) = \frac{a_z - \dfrac{\sigma_z \cdot \Delta t}{\varepsilon_0 n^2(i,j,k+1)}}{a_z + \dfrac{\sigma_z \cdot \Delta t}{\varepsilon_0 n^2(i,j,k+1)}} \cdot D_{1z}{}^{l-1}(i,j,k+1)$$

$$+ \frac{1}{a_z + \dfrac{\sigma_z \cdot \Delta t}{\varepsilon_0 n^2(i,j,k+1)}} \cdot \left[\Psi^{l}(i,j,k+1) - \Psi^{l}(i,j,k)\right]$$

$$\sigma_z(z) = \left(\frac{z}{d}\right)^m \sigma_{z\max} = -\left(\frac{z}{d}\right)^m \frac{n_z^{\,2}\varepsilon_0 c(m+1)\ln(R_0)}{2d}$$

$$+ \frac{1}{a_z + \dfrac{\sigma_z \cdot \Delta t}{\varepsilon_0 n^2(i,j,k+1)}} \cdot \left[D_{1z}{}^{l+1}(i,j,k+1) - D_{1z}{}^{l+1}(i,j,k-1)\right.$$

$$\left. - D_{1z}{}^{l-1}(i,j,k+1) + D_{1z}{}^{l-1}(i,j,k-1)\right]$$

$$\sigma_z(z) = \left(\frac{z}{d}\right)^m \sigma_{z\max} = -\left(\frac{z}{d}\right)^m \frac{n_z^{\,2}\varepsilon_0 c(m+1)\ln(R_0)}{2d}$$

$d = n_z \Delta z$: Thickness of *PML*, m: order

R_0: Reflection from *PML* at normal incidence

n_z=8, R_0=10^{-2}, m=4

Application of FDTD Method:

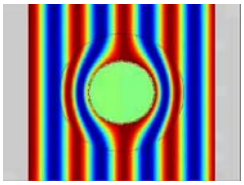

Eg. Invisible cloak. (by Dr. G. D. Chang, 張高德博士)

Eg. A laser beam passes a Fresnel's lens with $R_k=\sqrt{k\lambda f}$, k: integer, $\Delta n=n_2-n_1=1.5$.

(by J. –B. Huang, *et al*.)

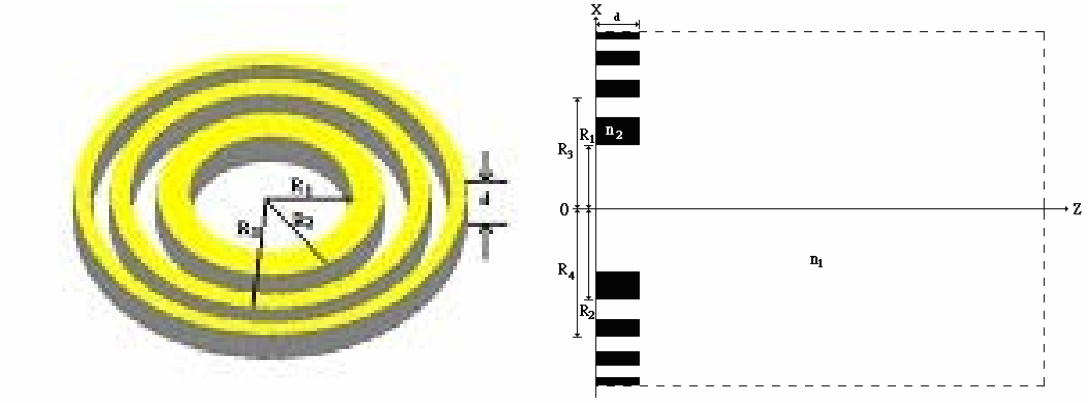

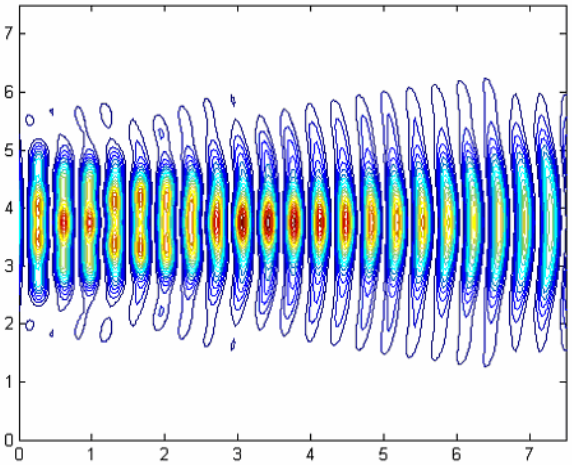

Eg. Laser beams passed microlenses composed of photonic crystals.

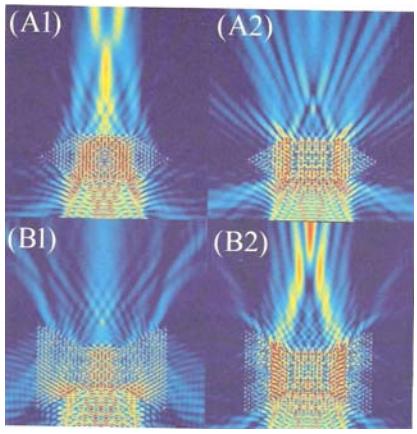

Eg. A laser beam passes a Fresnel's lens with n=1.57, λ=0.6μm. (by Y. –J. Lin)

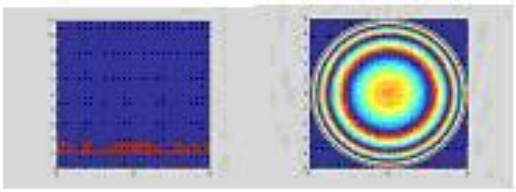

(Side view) (Top view)

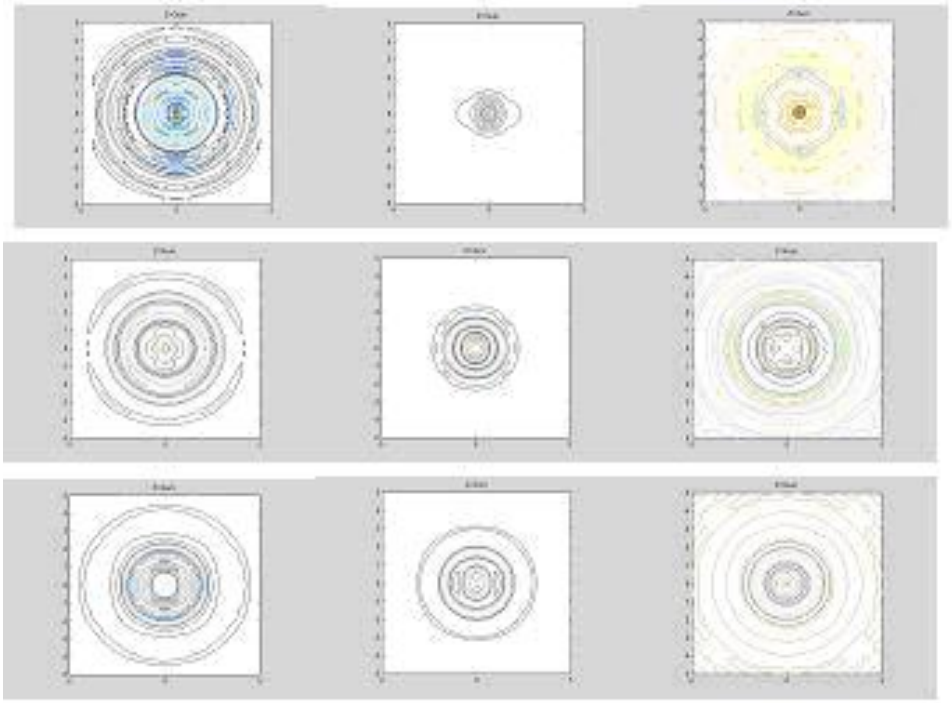

scalar *x*-polarized *y*-polarized

Eg. 3D Gaussian beams of w_0=2μ*m* through a conventional lens. (by K. –Y. Lee)

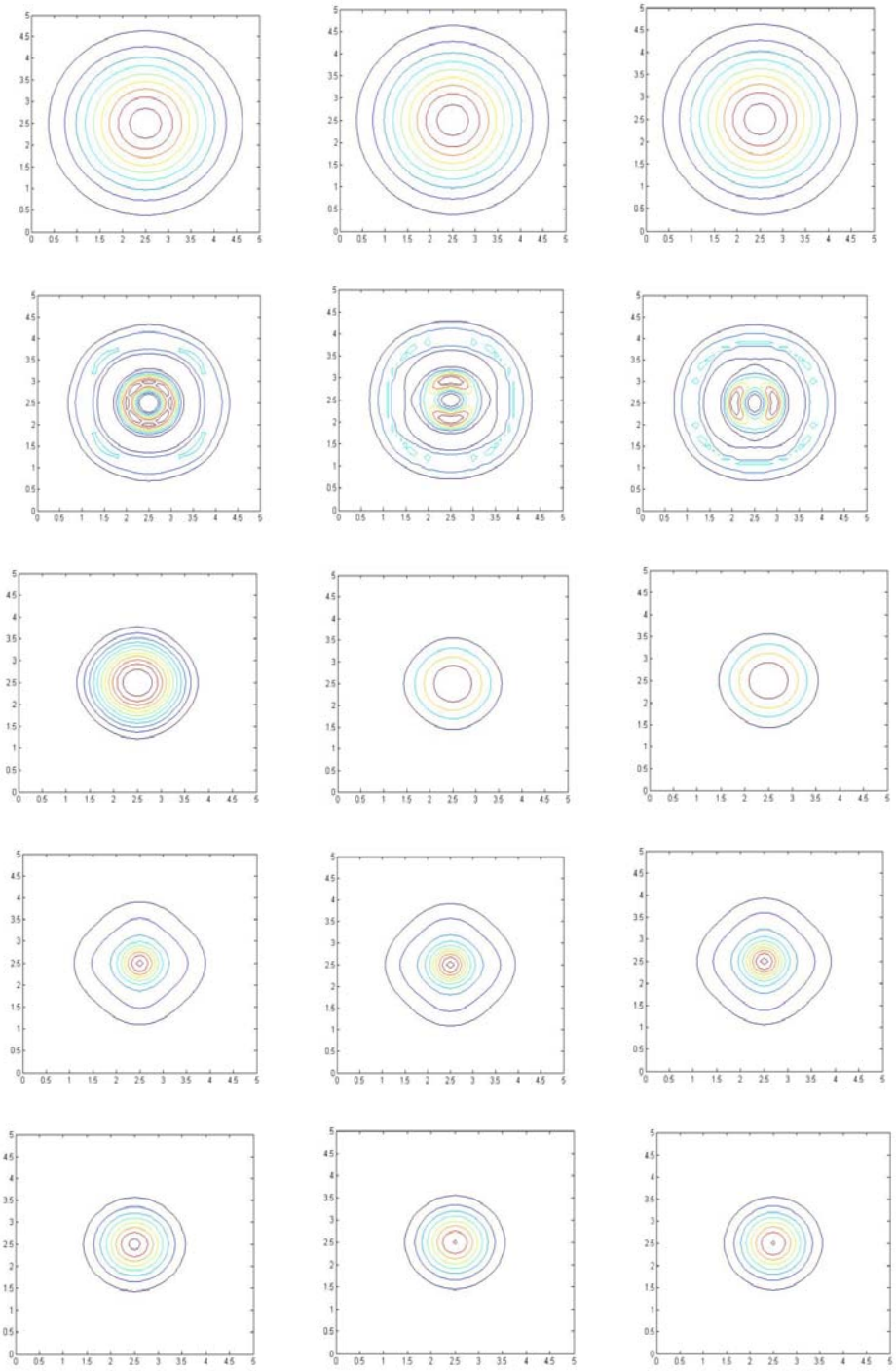

scalar *x*-polarized *y*- polarized

Appendix I-Diffractive Optics and Fresnel Lenses

繞射光學

- ❖ 研究如何利用光波繞射效應設計出所需的繞射光學元件而實現傳統光學元件所無法達到的特殊光學功能。
- ❖ 基於光波繞射理論為設計方法，而以半導體製程技術為主要的製作方法。
- ❖ 具有厚度薄、重量輕、結構緊湊並易於複製等優點並易與其它光電元件結合。

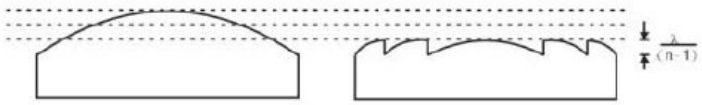

菲涅耳燈塔透鏡的直徑一般比它的焦距大許多

透鏡高3.7m ；寬1.8m ；焦距0.91m

傳統透鏡可利用Fresnel透鏡來減少厚度，而二進階光學則是利用二進階式(2, 4, 8. . .)的階層來近似Fresnel透鏡

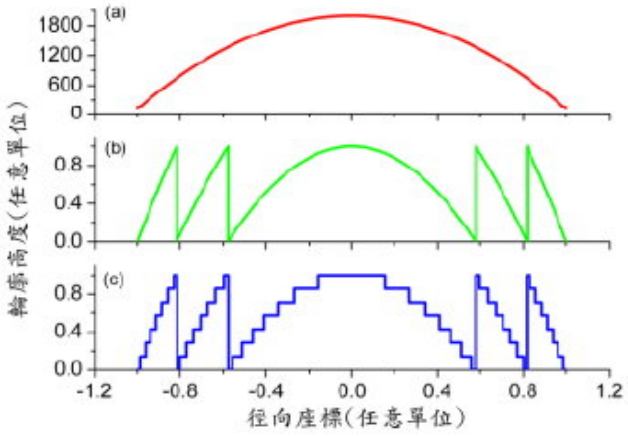

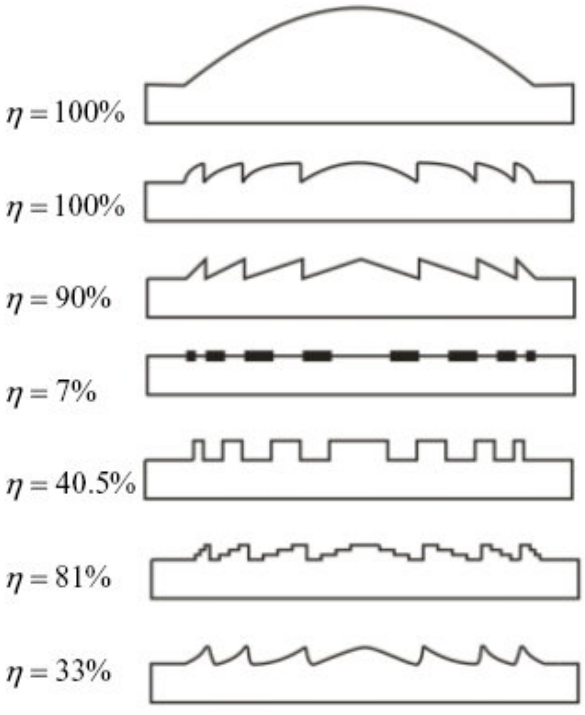

折射透鏡
(研磨製程)

閃耀型菲涅耳透鏡
(微影製程/鑽石車削)

閃耀型三角狀菲涅耳透鏡
(鑽石車削)

二階振幅型繞射透鏡
(微影製程)

二階相位型繞射透鏡
(微影/蝕刻製程)

多階近似相位型繞射透鏡
(微影/蝕刻製程)

全像繞射透鏡
(干涉微影/蝕刻製程)